LOW-FREQUENCY ELECTROMAGNETIC OSCILLATIONS OF THE EARTH-IONOSPHERE CAVITY

T. Madden
W. Thompson

September 22, 1964

Project NR-371-401

Geophysics Laboratory
Massachusetts Institute of Technology
Cambridge 39, Massachusetts

CLEARINGHOUSE FOR FEDERAL SCIENTIFIC AND TECHNICAL INFORMATION CFSTI
DOCUMENT MANAGEMENT BRANCH 410.11

LIMITATIONS IN REPRODUCTION QUALITY

ACCESSION # AD 607080

☑ 1. WE REGRET THAT LEGIBILITY OF THIS DOCUMENT IS IN PART UNSATISFACTORY. REPRODUCTION HAS BEEN MADE FROM BEST AVAILABLE COPY.

☑ 2. A PORTION OF THE ORIGINAL DOCUMENT CONTAINS FINE DETAIL WHICH MAY MAKE READING OF PHOTOCOPY DIFFICULT.

☐ 3. THE ORIGINAL DOCUMENT CONTAINS COLOR, BUT DISTRIBUTION COPIES ARE AVAILABLE IN BLACK-AND-WHITE REPRODUCTION ONLY.

☐ 4. THE INITIAL DISTRIBUTION COPIES CONTAIN COLOR WHICH WILL BE SHOWN IN BLACK-AND-WHITE WHEN IT IS NECESSARY TO REPRINT.

☐ 5. LIMITED SUPPLY ON HAND: WHEN EXHAUSTED, DOCUMENT WILL BE AVAILABLE IN MICROFICHE ONLY.

☐ 6. LIMITED SUPPLY ON HAND: WHEN EXHAUSTED DOCUMENT WILL NOT BE AVAILABLE.

☐ 7. DOCUMENT IS AVAILABLE IN MICROFICHE ONLY.

☐ 8. DOCUMENT AVAILABLE ON LOAN FROM CFSTI (TT DOCUMENTS ONLY).

☐ 9.

PROCESSOR: [illegible]

TSL-107-10/64

LOW-FREQUENCY ELECTROMAGNETIC OSCILLATIONS OF THE EARTH-IONOSPHERE CAVITY

T. Madden
W. Thompson

September 22, 1964

Project NR-371-401

Geophysics Laboratory
Massachusetts Institute of Technology
Cambridge 39, Massachusetts

ABSTRACT

The observational and theoretical work on the low frequency electromagnetic oscillations of the earth-ionosphere cavity, known as the Schumann resonances, is reviewed. Additional theoretical considerations are introduced that allow the models to incorporate all the important complications of the real ionosphere. The comparisons between the theoretical predictions and the observational data lead to implications about the structure of the very low ionosphere, and the geometry of ionospheric perturbations which are discussed.

INTRODUCTION

In recent years a growing interest has been developing in the geophysical implications of the electromagnetic resonances of the cavity formed between the earth and its ionosphere. The data that can be derived from passive observations of these resonances excited by the naturally occuring lightning discharges promises to add considerably to our knowledge of the properties of the ionosphere. There are several features of these observations that make them a unique way of studying the ionosphere. First of all, the frequencies, which start at about 8 cycles per second, are much lower than the frequencies otherwise available for making ionospheric radio measurements and therefore they are strongly influenced by lower regions of the ionosphere that are difficult to study by the standard rocket or ground based techniques.

Secondly, the measurements involve world wide properties of the ionosphere as the waves that are observed have travelled around the earth several times, so that all sections of the cavity can, in a sense, be monitored from a single observing site. A distribution of observing sites is necessary, however, to uniquely separate the geographical distributions of these properties. The measurements can also usually be made continuously so that it is possible to investigate some of the transient effects that involve the ionosphere.

The earlier work on this problem is reviewed in the first section. The electromagnetic properties of the iono-

sphere are examined briefly in the second section. The large variations of these properties with geographic position necessitates an extension of the earlier theoretical work in order to make quantitative use of the data. A technique to handle this problem is discussed in the third section. In the fourth section we compare the results of theoretical models with the existing observational data and consider some of the geophysical implications of these comparisons. Some further mathematical details are to be found in the appendix.

I. HISTORICAL REVIEW

The first ideas that an ionosphere was present above the earth's surface and capable of trapping electromagnetic energy was put forward in 1902 by Heavyside and Kennelly. Watson in two famous papers (Watson, 1918, 1919) developed some of the most important mathematical tools for dealing with a spherical wave guide, and a tremendous amount of literature is devoted to the propagation of electromagnetic waves through an earth-ionosphere wave guide (see Review article by Wait, 1963). It is not until 1952, however, that we find any literature concerning itself with the resonance of the entire wave guide system. Schumann is credited with first studying the theoretical aspects of this problem and also with König of first attempting to measure the resonant frequencies (Schumann, 1952, 1954). For this reason the phenomenon of the earth-ionosphere cavity resonances are known as the Schumann resonances.

The resonant frequencies are mainly determined by the size of the earth and the speed of light, but the ionospheric properties modify these frequencies to a certain extent. The lowest resonant modes are at sub-audio frequencies and far below the frequencies ordinarily used for radio communication. These frequencies lie at the low end of the range of frequencies that the radio people designate as E.L.F.

Lightning discharges provide a broad spectrum of energy at these frequencies and it is relatively easy to measure this background energy at any time. The spectrum of the lightning source is modified by the resonance properties of the earth-ionosphere cavity system, and this signature should be observed in the resulting noise signals. The number of lightning strokes occurring at any one time is in general too high to be able to distinguish at these frequencies the wave forms of individual flashes, and one must resort to measuring the power density spectrum of the background noise. It was not till Balser and Wagner's measurements (Balser and Wagner, 1960, 1962, 1963) that adequate analysis techniques were used to extract the resonance information from this background noise. By digitizing two hours worth of background noise received on a vertical antenna and numerically filtering the digital data they were able to identify the first five resonant modes and to estimate the Q of these modes from the shape of the power density spectrum. These preliminary results are shown in Figure 1. Balser and Wagner also had attempted to determine some of the higher modes (Balser and Wagner J. R. NBS., 1960) but their results were less statistically significant. They have continued this work using both digital and analogue techniques and have studied the time variations of the power in the resonant modes and of the frequencies of these modes.

The successful work of Balser and Wagner really marks

the beginning of a great interest in this phenomenon which is being pursued both theoretically and experimentally. (Benoit, 1962; Chapman and Jones, 1964; Galejs, 1961, 1962; Gendrin et Stefant, 1962; Harris and Tanner, 1962; Pierce, 1963; Polk and Fitchen, 1962; Raemer, 1961; Row, 1962; Rycroft, 1963; Thompson, 1962; Wait, 1964.)

Most of the theoretical efforts have been aimed at improving the mathematical models so as to better represent the actual ionosphere. Schumann, in his pioneering work, showed that the resonant frequencies for a perfectly reflecting ionosphere would be given by $f_n = \sqrt{\frac{n(n+1)}{\epsilon\mu}}/2\pi R$ resulting in frequencies of about 10.6, 18.4, 26.0, 35.5, and 41.1 for the first five modes. Schumann also considered the effect of a finite conducting ionosphere and showed that the resonant frequencies would be lowered and the Q reduced. Galejs considered the effect of an exponential conductivity profile in the ionosphere and showed that important energy losses occurred in the very low regions of the ionosphere. Thompson considered the influence of a vertical magnetic field and showed how the resulting anisotropic conductivity profoundly modified the cavity properties, especially at night. Wait, Galejs, and Harris and Tanner have made contributions toward treating the inhomogeneities of the wave guide system. None of these earlier treatments have involved the full complexity of the actual ionosphere.

Other theoretical efforts have been aimed at studying the effect of the lightning source statistics and their geographic distribution on the resulting observed noise spectra (Raemer,

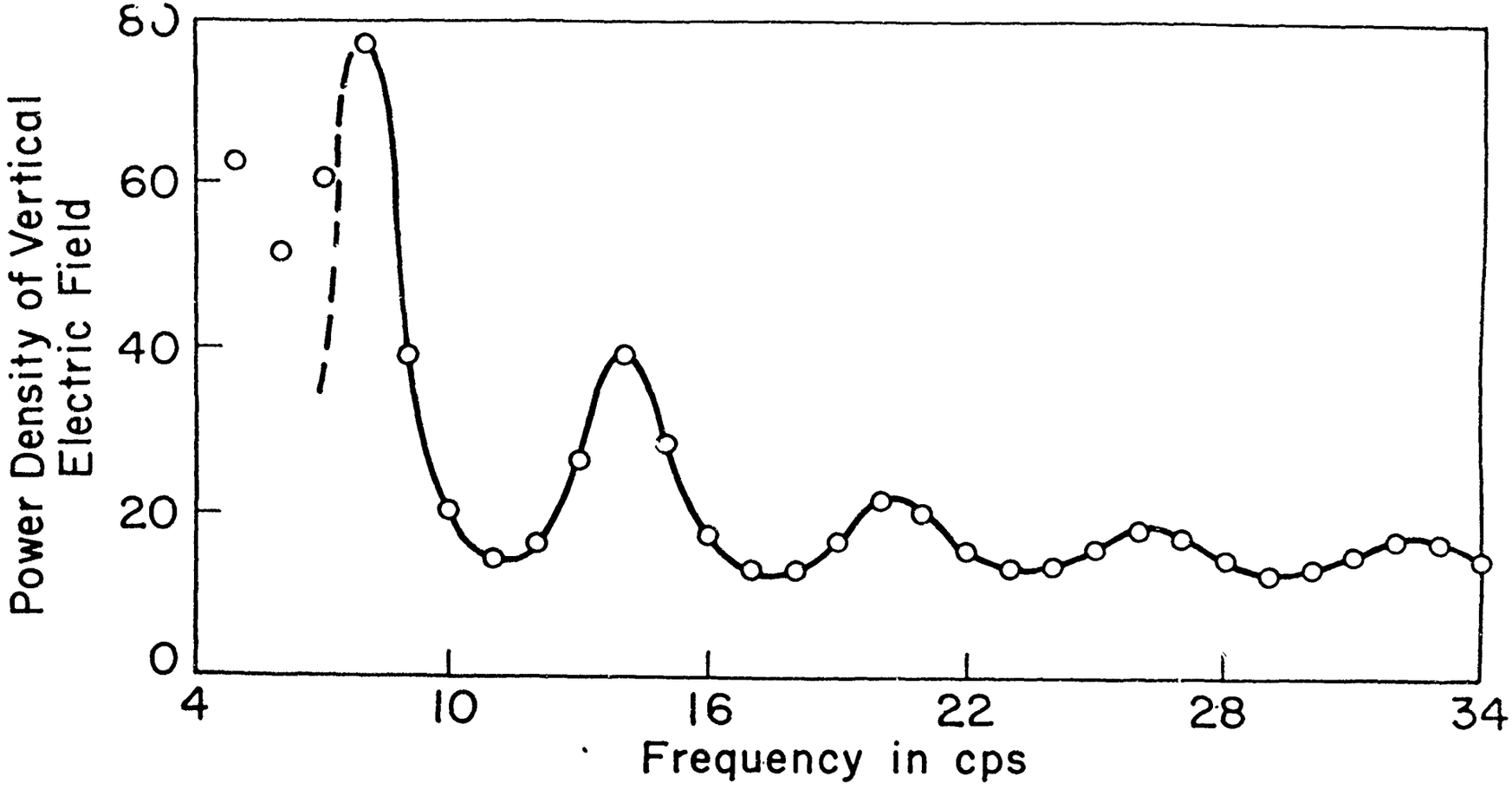

Composite spectrum of 10 12-minute records of ELF noise. Results reported by Balser and Wagner 1960

Figure 1 Experimental evidence of the existance of Schumann resonances

1961; Holzer, 1958; Pierce, 1963). There is some disagreement about the details of the source spectra. Lightning discharges are complicated phenomenon with several current surges of different time durations (Watt, 1960; Pierce, 1963). Most of the surges are rapid enough at the frequencies of interest here to be considered as impulse functions, but the correlations between repeated strokes modify the resulting spectra and enhance the low frequency end of the spectrum. Also, some long discharges are slow enough to limit the energy in the frequencies of the higher resonant modes. Since the observed spectra depends on the cavity properties and the source locations as well as the source spectra, it is not a trivial problem to resolve the source spectra from the observed Schumann resonances.

The experimental work is simple in principle, as the measurements are easy to make with our modern electronic technology, but a great deal of analysis is required to extract the information available in these measurements. The frequency analysis of the observed noise background is often done by digital computations, but this is restricted to spot data, as synoptic studies would be too expensive. Analogue techniques using banks of filters must be resorted to for extensive studies of the Schumann resonances. A popular way of presenting such analogue results are the time-frequency plots that the sonographs and other similar instruments can produce.

Observations are usually made with vertical antennas or with induction coils. The vertical antennas are omnidirectional receivers, while the induction coils can be oriented to receive a particular component of the magnetic field. The vertical antennas have the advantage, however, that they only respond to the TM modes which is the mode of the Schumann resonances. Signals that originate in the ionosphere, because of the reflection properties of the air layer, come down to the earth's surface essentially in the TE mode. These signals will not participate in the Schumann resonances, and could, if they are large enough, mask the resonance signals in the horizontal magnetic field components. The induction coils do have the advantage that they are more easily shielded from the weather, as rain or dew can short out the electric signals even when the antenna is enclosed in a radar dome. (Balser and Wagner, 1963). Because of the large vertical electric gradient in the air, there is always also the possibility that electric signals will be produced by modulations of the electrical conductivity of the air. This does not appear to mask the electromagnetic signals. Even the presence of local thunder activity does not mask the Schumann resonances if the energy of local lightning flashes is eliminated from the recordings by clipping (Wagner-personal communication).

Horizontal electric measurements can also be used, and they are closely related to the horizontal magnetic measurements. They are perhaps the easiest measurement to make,

but unfortunately, the most susceptible to man made interference. A very bad noise source are the subharmonics of the power line frequency. These peculiar signals are apparently due to non linear interactions between the generators of the power system, and unfortunately these frequencies fall right on top of some of the Schumann resonances. They are distinguished by the fact that they have a line spectra, but are not quite exact subharmonics, and when displayed on an oscilloscope the 60 cycle wave form is observed to drift slowly through the subharmonic wave form.

The experimental programs are still in the early stages, but several results have been reported. The original frequency structure of the Schumann resonances as reported by Balser and Wagner have been substantiated with minor changes by many observers. (Gendrin, 1962; Benoit, 1962; Chapman, 1964; Lokken, 1961; Rycroft, 1963) The general character of the amplitute pattern has been explained in terms of localization of most of the lightning activity in the equatorial continental regions at local afternoon times. (Balser and Wagner, 1962). Systematic shifts of the resonance frequencies that repeat on a daily basis have also been reported (Balser and Wagner, 1962). These variations amount to about 5 % of the frequency. Some frequency shift is to be expected as the source-receiver geometry changes throughout the day, but a systematic change in the cavity system cannot be ruled out because of the displacement of the magnetic pole from

the rotational pole. At present this data is only reported for New England so that it is difficult to untangle the two effects.

Sudden shifts of the Schumann resonances amounting to 5-7% also have been reported immediately following the Johnson Island high altitude nuclear explosion of July 9, 1962. These shifts were reported from both New England (Balser and Wagner, 1963) and France (Gendrin and Stefant, 1962) and there is no doubt that a systematic change in the earth-ionosphere cavity was involved.

A summary of some of these observations is given in Table I.

TABLE I

OBSERVATIONAL DATA CONCERNING SCHUMANN RESONANCES

Mode number	1	2	3	4
frequency in cps	8.0	14.0	20.0	26.5
Q	4	5	5	6
diurnal variations of f_n in cps	$\pm$0.2	$\pm$0.3	$\pm$0.5	$\pm$0.5
transient shift of f_n in cps following July 9, 1960 nuclear explosion as observed in France	-0.5	-0.5	-0.9	-0.9

TABLE I

OBSERVATIONAL DATA CONCERNING SCHUMANN RESONANCES

Mode number	1	2	3	4
frequency in cps	8.0	14.0	20.0	26.5
Q	4	5	5	6
diurnal variations of f_n in cps	±0.2	±0.3	±0.5	±0.5
transient shift of f_n in cps following July 9, 1960 nuclear explosion as observed in France	-0.5	-0.5	-0.9	-0.9

II LOW FREQUENCY ELECTROMAGNETIC PROPERTIES OF IONOSPHERE

The strong electromagnetic influence of the ionosphere arises from the presence of free electrons and ions. This ionization results from solar and cosmic irradiation and is the subject of intense study these days. A general understanding of the many factors that are involved has developed, but there is still a lack of adequate quantitative data, (see Review article by Reid, 1964) and many problems remain to be resolved. We are not primarily involved in this study with these problems of ionization, but eventually, of course, all the indirect methods of probing the ionosphere must lead to consistent models of this ionization. Later we shall see that the Schumann resonance data imposes strong limitations on the ionization levels that can be existing in the lower D or what is sometimes called the C region. In this section we wish to examine the behavior of sub-audio frequency electromagnetic waves in the environment of the atmosphere and ionosphere.

The electromagnetic waves of the Schumann resonances have the interesting property of exhibiting large parts of the entire spectrum of electromagnetic wave behavior as they propagate through the atmosphere and ionosphere, starting as classical electromagnetic waves in the atmosphere and ending as magnetohydrodynamic waves in the F regions and above. Because of this one must keep track of many ionospheric parameters, and the classical subdivisions of the ionosphere based

only on the electron concentrations lose their significance. Strictly speaking, the waves are not electromagnetic waves but plasma waves and involve the partial pressures of the plasma constituents as well as the electric and magnetic vectors. Plasma waves have been intensively studied during the past ten years, and one can now draw on a good understanding of their general properties. In the earth's ionosphere the acoustic waves have velocities so slow compared to the electromagnetic waves that they are largely uncoupled, and we can essentially ignore the pressure terms and consider the waves as simply electromagnetic waves. Also, because the ionosphere is a temperate plasma and our wavelengths are long compared to the critical microscopic lengths, the behavior of these waves is adequately described by Maxwell's equations. A complication arises from the anistropy of the ionospheric electric conductivity due to the presence of the earth's magnetic field. Since, at the Schumann resonance frequencies, conduction currents dominate over the displacement currents above about 60 KM, the anisotropy of the electrical conductivity profoundly alters the electromagnetic wave behavior beyond this altitude. The subject of plasma electromagnetic waves is extensively treated in many excellent texts (Ginzburg, Allis, Spitz) and numerous articles, and we shall only briefly review the points of interest to our problems.

To solve for the electrical conductivity a relationship is derived between J and E from the linearized equations of motion for the plasma constituants. In these equations

the frictional effects are usually represented in terms of an effective collision frequency between various constituants multiplied by their relative mean velocities. This concept is not really correct when the collision frequency depends on the velocity of the individual particles (Ginzburg, Katz) but the errors involved are within a factor of two and can usually be absorbed by making the effective collision frequency depend on the probing electromagnetic wave frequency.

The solution of these linear equations can be simplified by making use of the large ion to electron mass ratio to drop small terms. Depending on where in the calculations these approximations are made, different algebraic formula are obtained which are, however, numerically equivalent. The most commonly used formulas are given by

$$\sigma_0 = \frac{Ne^2}{m_e(\nu_{ei} + \nu_{en} - i\omega)} \tag{1}$$

$$\sigma_\perp = Ne^2\left\{\frac{\nu_{ei}+\nu_{en}-i\omega}{m_e\left[(\nu_{ei}+\nu_{en}-i\omega)^2+\omega_e^2\right]} + \frac{\nu_{in}-i\omega}{m_i\left[(\nu_{in}-i\omega)^2+\omega_i^2\right]}\right\} \tag{2}$$

$$\sigma_\times = Ne^2\left\{-\frac{\omega_e}{m_e\left[(\nu_{ei}+\nu_{en}-i\omega)^2+\omega_e^2\right]} + \frac{\omega_i}{m_i\left[(\nu_{in}-i\omega)^2+\omega_i^2\right]}\right\} \tag{3}$$

These equations assume that the plasma is electrically neutral and contains no negative ions.

σ_0 is the conductivity parallel to the magnetic field, $\sigma_\perp$ the conductivity perpendicular to the field, and σ_x the Hall conductivity, all given in mhos/meter

ω is the radio wave frequency in radians per second

ω_e is the electron gyro frequency in radians per second

ω_i is the ion gyro frequency in radians per second

N is the electron and positive ion concentration in M^{-3}

$\nu_{ei}, \nu_{en}, \nu_{in}$ are the effective collision frequencies between electrons and ions, electrons and neutrals, and ions and neutrals respectively in sec^{-1}

A numerically equivalent expression that is more useful for our purposes is given as

$$\sigma_x = \sigma_0 \frac{W}{(1+W^2)(1+\Omega^2)} \qquad W = \frac{\omega_e}{\nu_{ei}+\nu_{en}-i\omega} \tag{4}$$

$$\sigma_\perp = \sigma_0 \frac{1+W\Omega}{(1+W^2)(1+\Omega^2)} \qquad \Omega = \frac{\omega_i}{\nu_{in}-i\omega} \tag{5}$$

From (4) and (5) we see that three distinctly different regions exist with which we associate three different regions of electromagnetic wave behavior.

(a) $|W|, |\Omega| \ll 1$ $\qquad \sigma_x \ll \sigma_\perp \approx \sigma_0$

(b) $|W| \gg 1, |\Omega| \ll 1$ $\qquad \sigma_\perp \ll \sigma_x \ll \sigma_0$

(c) $|W|, |\Omega| \gg 1$ $\qquad \sigma_x \ll \sigma_\perp \ll \sigma_0$

This representation emphasizes the role of the collision frequencies in determining the wave types. At the lower Schumann resonances ω is much less than ω_e and somewhat less than ω_i, so that we pass from region a to b to c as $\nu_{ei} + \nu_{en}$ and ν_{in} become less than ω_e and ω_i respectively. (The ion gyro frequency is about 30-50 cycles per second in the ionospheric regions of interest to us here.) Tables II and III give mid-latitude estimates of these conductivities at 7.5 cps and include the displacement contribution.

In order to study the electromagnetic wave types a plane wave solution to Maxwell's equations is sought. When $W \ll 1$ the conductivity is isotropic and we have

$$k^2 \cong \epsilon\mu\omega^2 + i\mu\omega\sigma_0 \qquad (6)$$

This expression is valid up to heights of about 60 KM in the ionosphere. At these lower ionospheric levels we cannot use (1) to calculate σ_0 because the ion populations are much greater than the electron populations, and their contributions to σ_0 cannot be ignored. In fact, below about 40 KM in the day and 50 KM at night the electrical conductivity is predominantly ionic.

As long as $|i\mu\omega\sigma_0| \ll \epsilon\mu\omega^2$ the phase velocity of the waves are essentially equal to the speed of light and

TABLE II

MID-LATITUDE DAYTIME COMPLEX CONDUCTIVITY PROFILE

Electrical Conductivity at 7.5 cps Including Displacement Contribution in mhos/meter

h in km	σ_0	$\sigma_\perp$	σ_x
10	-4.21×10^{-10}	-4.21×10^{-10}	6.8×10^{-17}
18	$(.01 - 4.21) \times 10^{-10}$	$(.01 - 4.21) \times 10^{-10}$	7.3×10^{-16}
27	$(.06 - 4.21) \times 10^{-10}$	$(.06 - 4.21) \times 10^{-10}$	1.3×10^{-14}
39	$(.26 - 4.21) \times 10^{-10}$	$(.26 - 4.21) \times 10^{-10}$	1.3×10^{-13}
45	$(.43 - 4.21) \times 10^{-10}$	$(.43 - 4.21) \times 10^{-10}$	5.6×10^{-13}
52	$(1.9 - 4.21) \times 10^{-10}$	$(1.9 - 4.21) \times 10^{-10}$	9.2×10^{-12}
60	$(1.1 - .041) \times 10^{-8}$	$(9.9 - .421) \times 10^{-9}$	2.9×10^{-9}
69	5.6×10^{-7}	2.0×10^{-7}	2.7×10^{-7}
78	2.0×10^{-5}	4.8×10^{-7}	3.0×10^{-6}
89	8.6×10^{-4}	9.8×10^{-7}	2.5×10^{-5}
100	2.4×10^{-2}	$(1.0 + .021) \times 10^{-5}$	1.7×10^{-4}
113	$(8.8 + .021) \times 10^{-2}$	$(4.7 + .221) \times 10^{-5}$	2.6×10^{-4}
127	$(3.7 + .021) \times 10^{-1}$	$(2.1 + .141) \times 10^{-4}$	$(3.1 - .341) \times 10^{-4}$
142	$(1.8 + .021) \times 10^{0}$	$(2.8 - 1.41) \times 10^{-4}$	$(.59 - 1.21) \times 10^{-4}$

TABLE III

MID-LATITUDE NIGHTIME COMPLEX CONDUCTIVITY PROFILE

Electrical Conductivity at 7.5 cps Including Displacement Contribution in mhos/meter

H in Km	σ_o	$\sigma_\perp$	σ_x
8	$-4.2i \times 10^{-10}$	-4.21×10^{-10}	2.0×10^{-17}
14	$-4.2i \times 10^{-10}$	-4.21×10^{-10}	9.1×10^{-17}
21	$(.02 - 4.2i) \times 10^{-10}$	$(.02 - 4.21) \times 10^{-10}$	4.8×10^{-16}
28	$(.06 - 4.2i) \times 10^{-10}$	$(.06 - 4.21) \times 10^{-10}$	3.0×10^{-15}
36	$(.17 - 4.2i) \times 10^{-10}$	$(.17 - 4.21) \times 10^{-10}$	2.4×10^{-14}
45	$(.31 - 4.2i) \times 10^{-10}$	$(.31 - 4.21) \times 10^{-10}$	1.4×10^{-13}
55	$(1.0 - 4.2i) \times 10^{-10}$	$(1.0 - 4.21) \times 10^{-10}$	3.7×10^{-12}
66	$(2.5 - .42i) \times 10^{-9}$	$(2.0 - .42i) \times 10^{-9}$	1.0×10^{-9}
77	2.5×10^{-7}	$(1.5 - .04i) \times 10^{-8}$	6.0×10^{-8}
90	3.9×10^{-5}	$(4.2 - .04i) \times 10^{-8}$	1.1×10^{-6}
105	2.4×10^{-3}	$(7.3 + .16i) \times 10^{-7}$	8.4×10^{-6}
120	1.1×10^{-2}	$(2.9 + .23i) \times 10^{-6}$	$(8.0 - .19i) \times 10^{-6}$
137	$(6.1 + .22i) \times 10^{-2}$	$(4.5 - 1.1i) \times 10^{-6}$	$(4.1 - 1.8i) \times 10^{-6}$
156	$(2.5 + .35i) \times 10^{-1}$	$(1.5 - 2.7i) \times 10^{-6}$	$(-4.8 - 7.1i) \times 10^{-7}$
177	$(4.6 + 1.2i) \times 10^{-1}$	$(.68 - 2.9i) \times 10^{-6}$	$(-6.5 - 3.1i) \times 10^{-7}$
200	$(8.1 + 3.8i) \times 10^{-1}$	$(.28 - 2.9i) \times 10^{-6}$	$(-6.7 - 1.2i) \times 10^{-7}$
226	$(1.1 + 1.4i) \times 10^{0}$	$(.17 - 3.0i) \times 10^{-6}$	$(-6.7 - .73i) \times 10^{-7}$
253	$(.54 + 2.2i) \times 10^{0}$	$(.10 - 3.2i) \times 10^{-6}$	$(-6.8 - .42i) \times 10^{-7}$
284	$(5.3 + 8.1i) \times 10^{0}$	$(.03 - 1.6i) \times 10^{-5}$	$(-3.2 - .11i) \times 10^{-6}$

the wave fronts will be moving horizontally. A small amount of damping due to the conductivity term can become important, however, because of the large distances that the waves are travelling. Above about 50-60 KM the conductivity term begins to dominate over the displacement current term, and the decreasing phase velocity forces the wave normals to become more nearly vertical. The damping is much heavier, but the waves travel only a relatively short distance through this highly damped region. As the waves move slightly higher in the ionosphere the electron collision frequency decreases enough to allow the electron motions to become circular, and the electrical conductivity becomes anistropic. It is necessary in order to study the wave behavior to develop the full expression for the propagation constants.

The expression for the general case is very complex, but we can recover a simple expression making two more approximations that hold for most of the Schumann resonance waves above about 50 KM. If we ignore displacement currents and if we make the quasi-longitudinal approximation $\sigma_0 \cos^2\theta \gg \sigma_\perp \sin^2\theta$ where θ is the angle the propagation vector makes with the magnetic field, we obtain as a solution

$$k^2 \simeq i\mu\omega \left[\sigma_\perp \left(\frac{1+\frac{1}{\cos^2\theta}}{2} \right) \pm \frac{1}{2} \sqrt{\sigma_\perp^2 \left(1-\frac{1}{\cos^2\theta}\right)^2 - 4\,\frac{\sigma_x^2}{\cos^2\theta}} \right] \quad (7)$$

Above about 80 KM σ_o is so much greater than $\sigma_\perp$ that the quasi-longitudinal approximation holds for the Schumann resonance waves everywhere except right on the magnetic equator. At lower altitudes the approximation is valid in a smaller region within 30° latitude of the magnetic poles.

From Tables II and III we see that $\sigma_x \gg \sigma_\perp$ in the region between 75 and 110 KM and then we can set

$$k^2 \cong \mp \frac{\mu\omega\sigma_x}{\cos\theta} \qquad (\cdot)$$

These are the waves we usually associate with whistlers. The mode associated with the top branch is essentially an evanescent wave. It is often called the ordinary wave in the whistler notation, and is polarized opposite to the electron rotation. The other branch gives us the whistler mode, which tends to be guided by the magnetic field and propagates with a polarization in the same sense as the electron rotation. This wave propagates with little damping in this region of the ionosphere.

Above 140 KM we find the ion collision frequencies are small enough compared to the ion gyro frequencies to have $\sigma_\perp > \sigma_x$

Under these conditions

$$k^2 \cong \begin{matrix} i\mu\omega\sigma_\perp \\ i\mu\omega\sigma_\perp/\cos^2\theta \end{matrix} \qquad (9)$$

These can be rewritten using (1) and (5) to give the more familiar form when $\nu_{in} \ll \omega$

$$k^2 \cong \begin{matrix} \dfrac{\omega^2\mu\rho_{ion}}{B_o^2} \\ \dfrac{\omega^2\mu\rho_{ion}}{B_o^2\cos^2\theta} \end{matrix}$$

These are the Alfven modes that arise when the sound velocity is assumed negligible. The first branch is often called the ordinary wave in the magnetohydrodynamic notation although it is the same branch that was called extraordinary in the magneto-ionic notation. A less confusing notation is to call the top branch the fast Alfven wave, and the bottom branch the slow or guided Alfven wave. Both waves propagate with little damping, and the guided wave is strongly guided by the magnetic field. At the Schumann resonance frequencies σ_x cannot really be ignored compared to $\sigma_\perp$ and some modification of the pure Alfven wave behavior results. These waves still propagate with little damping, however, beyond about 150 KM.

In the region between 110 and 140 KM the wave types are neither Alfven like nor whistler like. Allis and Stix refer to this region as the region of the lower hybrid resonant

frequency, but this terminology loses its meaning when the collision frequencies are important parameters as they are in the ionosphere at the Schumann frequencies. This region represents another zone of intense damping. This region also accounts for most of the damping of the micropulsation energy that is observed on the earth's surface.

Thus we find the ionosphere subdividing itself into regions according to the electromagnetic wave behavior at the Schumann frequencies. The physical parameters that determine these regions are the effective collision frequencies of the electrons and the ions rather than the electron densities. The overall behavior of the cavity still depends on all the parameters. The theory for predicting collision frequencies is somewhat stronger than the theory for predicting electron and ion densities as the important constants are better known, so that the information derived from the observations of the Schumann resonances will still most profitably be used to study the ionization densities.

III. MATHEMATICAL FORMULATION OF THE SCHUMANN RESONANCE PROBLEM

The earlier reported theoretical work on the Schumann resonance problem has been limited to treating ionospheric models that varied with altitude but not with geographic position. This work has helped us to gain a general picture of the effect of the ionosphere, but we cannot really make quantitative use of the Schumann resonance data until our theoretical models can include the geographical variations as well as the vertical variations of the ionosphere. Suggestions on procedures to be used to attack this problem have been made (Buchsbaum, 1960; Galejs, 1962; Harris, 1962; Wait, 1964a). In this section we wish to discuss a practical method of setting up such models, and also review the more classical formulations.

The Schumann resonance problem can be approached either as a Green's function problem in which the response of the cavity to a variable frequency source is studied, or as a characteristic frequency problem. The characteristic frequencies are those frequencies (which in real problems are usually complex valued) that allow solutions of the homogeneous equations i.e. no source terms. There is, of course, a very close connection between these methods. The theoretical results that are discussed in the next section were derived from a Green's function approach.

The Greens function problem in these coordinate systems where the equations are separable can be handled by straightforward and well documented eigenfunction techniques. (Morse and Feshbach, 1953; Sommerfeld, 1949) The procedure consists of defining a surface of the coordinate system on which the source is located and developing the source singularity in terms of the eigenfunctions associated with that surface. The function defining the behavior of the solution in the remaining coordinate is not an eigenfunction, but since there are always independent solutions, the remaining boundary conditions can be satisfied by a proper balance of these independent solutions. In many practical problems there are several ways of defining the surface so that different formulations of the problem result, and these different formulations lead to different physical interpretations as well as different numerical procedures. The eigenfunctions act like standing waves but otherwise they have no wave propagation properties. In fact the same eigenfunctions often appear in potential problems as do in wave propagation problems. The propagation wave behavior is only seen in the coordinate direction that is perpendicular to the surface on which the source was defined.

In spherical problems the defining surfaces most often used are the surfaces $R = R_0$ and $\Theta = 0$ (assuming the source is at the pole). In the former case the eigenfunctions are $\sin, \cos m\phi$ and $P_n^m(\cos\theta)$. The wave propagation behavior is exhibited in the R direction by the spherical

bessel functions $h_n^1(kR)$ and $h_n^2(kR)$. In the latter case the eigenfunctions are $\sin, \cos m\phi$ and $h_{\nu_n}^1(kR)$, $h_{\nu_n}^2(kR)$, where ν_n are complex values that give the radial functions proper boundary behavior. (Somerfeld, 1949) The wave propagation behavior is exhibited in the θ direction by the Legendre functions $P_{\nu_n}^m(-\cos\theta)$, $Q_{\nu_n}^m(-\cos\theta)$.

The former approach using spherical surface harmonics is more familiar and therefore more often used. However, in a problem involving propagation of waves around the earth it would appear more logical to use the latter approach. Watson (Watson, 1919) showed how one could transform a solution in the θ harmonics into one in the radial harmonics and that the latter representation was indeed much more efficient for many computational purposes. (see also Bremmer, 1949). The radial eigenfunctions that arise in this form are the wave guide modes.

Both types of solutions may be exhibited in a single integral which has the form (Wait, 1962; Bremmer, 1949)

$$U = \int_C \frac{f(\nu)}{\sin \nu\pi} P_\nu(-\cos\theta)\, d\nu \qquad (10)$$

The contour C encloses the poles of $\sin^{-1}\nu\pi$ and gives the spherical harmonic series representation. The contour can also be deformed so that the value of the integral is given instead by the residues of the poles of $f(\nu)$,

which are the radial eigenfunctions or the wave guide mode solutions. This is the transformation that is called the Watson transformation.

The characteristic frequency determination essentially merges these two approaches since the characteristic solutions are eigenfunctions in all the coordinate directions. (See also Bremmer, 1949; Wait, 1964.) If we consider the integrand (10) as the frequency ω is varied a pole of $f(\nu)$ at certain values of ω will merge with a pole of $\sin^{-1}\nu\pi$, ie. at $\nu = n$. The set of these frequencies are the characteristics frequencies or free oscillations of the system and would cause the integral (10) to diverge since a source term is implied in the representation. The real part of these characteristic frequencies are the resonant frequencies of the system, and the imaginary part of the characteristic frequency can be used to estimate the Q of the system

$$Q_n \cong \frac{\mathrm{Re}\ \omega_n}{2\,\mathrm{Im}\ \omega_n} \tag{11}$$

The meaning of the Q of a system tends to be a matter of definition. The more rigorous definitions involving the rate of energy dissipation are not often amenable to direct observation especially in continually excited systems, so that other observable quantities are used. The most often used quantity is the width of the observed resonance peak in the

power spectrum. For simple oscillating systems setting $Q = \frac{f_n}{\Delta f}$, where Δf is the separation of the half power points, is consistant with the definitions $\frac{1}{Q} = \frac{1}{2\pi} \frac{d \ln E}{d \text{ cycle}}$ as well as $Q = \frac{Re\, \omega_n}{2\, Im\, \omega_n}$.

When the Q is high these definitions are also consistant for any system. Practical difficulties arise when the Q is low enough to merge neighboring peaks in the power spectrum. In such cases the half power widths give an underestimate of the other two definitions of Q. It is very likely that this occurs in analysing the Schumann resonance peaks.

These analytic approaches that have been outlined are limited to models that allow our equations to separate. Unfortunately, some of the most interesting aspects of the actual earth-ionosphere cavity are complications that destroy this simiplicity. The influence of the magnetic field which is so very important in the night time ionosphere prevents the equations from separating in spherical coordinates unless the magnetic field is vertical. (Thompson, 1962.) The day-night and latitude asymmetries introduce further complications. If, however, we are to make quantitative use of the observations of the Schumann resonances we must find a practical way of incorporating all these complications into our mathematical models. A brute force attack on the problem is difficult because of the strong three dimensional charac-

ter of the problem. It turns out, however, that the problem can be broken down into two steps, each of which is fairly straightforward and conveniently organized for actual computations. The technique is essentially based on the use of transmission line equivalences to waveguide propagation, a concept that is used widely and very successfully by the microwave circuit people in handling very complicated waveguide problems (Montgomery, et al, 1948). The power of the method derives from the fact that any waveguide mode can be represented as propagation along a transmission line, and this representation is exact as long as only one waveguide mode is involved. In such a case the waveguide behavior can be reduced to a problem in circuit theory. When other modes are involved and the modes couple together at boundaries or interfaces of the system, some further complications are introduced. The beautiful advantage of these methods in the Schumann resonance problem comes about because at the frequencies of interest only the principle or TEM mode can propagate without very severe damping.

If we consider the field due to a point source in a waveguide, it can be represented as a contour integral in which the poles of the integrand represent the waveguide mode contributions and the branch cut represents the essentially spherically spreading wave energy and the near field. This breakup is often described as the discrete and continuous spectra (Brekhovskiki, 1960). The continuous spectra becomes

negligible compared to the waveguide modes at distances large compared to the waveguide height (Pekeris, 1948). When the height of the guide is less than a half wave length only the zeroth order modes can propagate without severe damping. For the Schumann resonances the wavelengths are fractions of the earth's circumference, while the height of the guide is only 50 to 60 KM, so that the higher order modes are damped out in distances of a few hundred kilometers. The energy that is observed at the resonant frequencies has travelled around the earth several times so that the continuous spectra is also negligible. Thus the wave energy is essentially confined to a single mode, the TEM or zeroth order TM mode.

For each such mode the relationship between the transverse components of E and H as described by Maxwell's equations are of the same form as the relationship between voltage and current in a transmission line. By proper normalization of the transmission line parameters it is also possible to make the energy flow along the transmission line equivalent to the energy flow along the waveguide. If only one mode is involved a properly normalized transmission line is an exact equivalent of the actual waveguide.

Consider propagation along a guide in the X direction of a TEM mode with no y dependence. From Maxwell's equations

we write

$$\frac{\partial H_y}{\partial x} = (\sigma - i\epsilon\omega) E_z \tag{12}$$

$$\frac{\partial E_z}{\partial x} = -i\mu\omega H_y + \frac{\partial E_x}{\partial z} \tag{13}$$

$$= -i\mu\omega H_y - \frac{1}{(\sigma - i\epsilon\omega)} \frac{\partial^2 H_y}{\partial z} \tag{14}$$

Along a transmission line we have

$$\frac{dV}{dx} = -Z I \tag{15}$$

$$\frac{dI}{dx} = -Y V \tag{16}$$

Z is the series impedances and Y the shunt admittance per unit length. Waves propagate along such a line with a propagation constant given as

$$k = -i\sqrt{Z Y} \tag{17}$$

The characteristic impedance of the line is given as

$$Z_{charact} = \sqrt{Z/Y} \tag{17}$$

In order to equate the energy flows we set

$$V = \int_0^{Alt} E_z \, dz \tag{19}$$

$$I = -H_y \tag{20}$$

Alt is taken as the height where E_z essentially disappears so that

$$VI^* = \int_0^{\infty} \int_0^{l} (E \times H^*) \cdot (dz \, dy) \tag{21}$$

(H_y is essentially constant in the range $z = 0, Alt$ for the TEM mode)

The energy flow along the ground is so small we take the bottom as on the earth's surface. In a microwave guide Alt is simply the height of the guide, but in the ionospheric guide the upper walls are diffuse. Because of the exponential increase of conductivity with height, and the accompanying rapid disappearance of E_z it will be accurate enough to take Alt as the height where the conductivity, $\sigma_o = \epsilon\omega$ and assume that

$$\int_0^{Alt} (\sigma - i\epsilon\omega) E_z \, dz = -i\epsilon\omega \cdot Alt \cdot E_z(0)$$

Now from (12) and (14) we can write

$$A\ell\tau \frac{dI}{dx} = i\epsilon\omega V \tag{22}$$

$$\frac{dV}{dx} = \left[i\mu\omega . A\ell\tau - f(0) \right] I \tag{23}$$

$f(0)$ is a correction due to $\int_0^{A\ell\tau} \frac{1}{\sigma - i\epsilon\omega} \frac{\partial^2 H_y}{\partial z^2} dz$

Now we can identify Y and Z with the parameters of the waveguide as

$$Y = - i\epsilon\omega / A\ell\tau \tag{24}$$

$$Z = - \frac{k_x^2}{Y} = k_x^2 A\ell\tau / i\epsilon\omega \tag{25}$$

k_x is the propagation constant of the waveguide mode and from (17) we see it will also be the propagation constant of the transmission line. The correction factor $f(0)$ is taken account of by the value of k_x . For a lossless guide the TEM mode propagates with the velocity of light and $k_x^2 = \epsilon\mu\omega^2$. For such a guide Z is represented by inductive elements and Y is represented by capacitive elements. In the actual earth ionosphere guide, the leakage of energy out of the guide leads to an added resistive component in Z , and the dissipation of energy in the guide leads to an added conductive component in Y .

The continuity conditions for V and I are the same as those for E_z and H_y, so that as long as the waveguide has constant dimensions the analogy between the two systems will be correct. Even when the dimensions of the waveguide change, the analogy holds as long as other modes are not generated by these changes. When sudden discontinuities arise in the guide it is usually necessary to introduce other waveguide modes in order to satisfy the boundary conditions. When these modes are non-propagating their effect can be represented by an added shunt reactance, but to determine the value of the reactance one must solve a boundary value problem (Montgomery, 1948). For gradual changes of the waveguide, this effect is unimportant.

The parameters of the equivalent transmission line also depend on the height of the guide, so that changes in the ionospheric height will cause impedance changes in the equivalent transmission line and these changes will modify the resulting propagation. In order to demonstrate that these impedance changes correctly simulate the effects of an actual gradual change of ionospheric height, let us consider a tapered guide or a sectorial horn for which the exact solutions of the TEM mode are known (Slater, 1959). The walls of such a waveguide are formed by the surfaces $\theta = \theta_1$ and $\theta = \theta_2$ in cylindrical coordinates. The TEM mode is represented by

$$H_z = A J_o(k\rho) + B N_o(k\rho)$$

(26)

$$E_\theta = -\frac{i\mu\omega}{k}\left[A\bar{J}_o'(k\rho) + BN_o'(k\rho)\right] \tag{27}$$

Because of the change of height as we move out along the guide (height is defined here as the arc length along ρ = const) the equivalent transmission line parameters are given as

$$Z = Z_o\,\rho\Delta\theta \tag{28}$$

$$Y = Y_o/\rho\Delta\theta \tag{29}$$

The transmission line equations are thus given as

$$\frac{dV}{d\rho} = -Z_o\,\rho\Delta\theta\,I \tag{30}$$

$$\frac{dI}{d\rho} = -\frac{Y_o}{\rho\Delta\theta}\,V \tag{31}$$

$$\therefore \frac{d^2I}{d\rho^2} = \left(\frac{Y_o}{\rho^2}V - \frac{Y_o}{\rho}\frac{dV}{d\rho}\right)\frac{1}{\Delta\theta} = -\frac{1}{\rho}\frac{dI}{d\rho} + Z_oY_o\,I \tag{32}$$

Since $Y_o Z_o = -k^2$ we have

$$\frac{1}{\rho}\frac{d}{d\rho}\left(\rho\frac{dI}{d\rho}\right) + k^2 I = 0 \tag{33}$$

$$I = AJ_o(k\rho) + BN_o(k\rho) \tag{34}$$

In this case we get the exact solution with our transmission line equivalence. This is so because no other waveguide modes were needed to satisfy the boundary conditions. For a varying taper this would not be true, but as long as the change of the taper is gradual the errors involved in neglecting the higher order modes are very small (Slater, 1959.)

Harris and Tanner (Harris, 1962) proposed an interesting analytic technique to handle waveguide inhomogenieties, but their method does not take account of changes of ionospheric height and thus does not properly keep track of the waveguide impedances.

The generation of other modes depends on the mismatch of the E and H components at the point where the guide properties change, and these mismatches have a $(1-\cos\delta\theta)$ like dependance where $\delta\theta$ is the change of angle involved. Thus the criteria for ignoring mode coupling involves the waveguide changing its shape slowly compared to the height of the guide. It is important to note that the transmission line equivalence does not depend on the assumption that the waveguide properties change slowly compared to a wavelength,

which is a necessary condition for the W.K.B. approximations which have been used to treat V.L.F. propagation in non-uniform waveguides (Wait, 1964a). The wavelengths of the Schumann resonance frequencies are actually much longer than the lengths of the transition zones separating the day and night ionospheres for example, and these changes can, therefore, set up partial reflections which are accounted for by the transmission line equivalences, but are unaccounted for in the W.K.B. approximations.

This all indicates that we can accurately describe the propagation properties of a section of the earth-ionosphere waveguide for the Schumann resonance problem in terms of two parameters such as the characteristic impedance of the guide and its propagation constant. To determine these parameters for a section of the earth ionosphere waveguide we must concern ourselves with the ionospheric structure and the magnetic field strength and its orientation. This, however, will only involve us with a one-dimensional problem as the transmission line equivalence allows us to separate out this section of the waveguide from the rest of the system. In order to solve the one-dimensional problem we have recourse to many techniques. The method used in this study involved a cylindrical geometry, and the air and ionosphere were described by a large number of layers of constant properties. We shall leave the description of the method actually used

to obtain solutions for the appendix. Many solutions must be carried out in order to get an accurate parameterizatio: for all the various sections of the earth-ionosphere system.

We have been using the term "transmission line" which is a one-dimensional concept, but in this particular problem we are really dealing with a two-dimensional transmission surface. This means that the surface impedance $\mathcal{Z}$ must be a 2nd order tensor, the principle axes of the tensor being oriented by the earth's magnetic field. Actually, the one-dimensional solutions showed that some TE mode was produced by the twisting effect of the magnetic field on the electromagnetic waves in the ionosphere so that $\mathcal{Z}$ should really be considered as a 4th order tensor. The amount of energy involved in this other mode was very small, however, and even the anisotropy of $\mathcal{Z}$ was minor so that $\mathcal{Z}$ can for most purposes be considered a scalar. The anisotropy of $\mathcal{Z}$ is not a complication as long as our axes are aligned with the principal axes of $\mathcal{Z}$.

Once the appropriate properties of the transmission surface are determined, there still remains the problem of solving for the response of this transmission surface to lightning excitation. This is now only a two-dimensional problem and is far simpler to deal with than the original three-dimensional problem. The computations in this study were done by solving a two-dimensional network that was the lumped circuit representation of the transmission surface equations. A schematic

representation of such a network is shown in figure 2. The methods of computation are discussed in the appendix.

It would also be possible to obtain analytic solutions of the transmission surface equations by perturbation techniques, although we did not use this approach in our computations.

In order to gain some insight on the behavior of an equivalent circuit representation, let us consider a uniform earth-ionosphere model. The network representing the transmission surface will be set up along latitude and longitude lines. The impedances connecting the nodes together will be proportional to the distance between the nodes and inversely proportional to the width of surface it is representing. The admittances connecting the nodes to ground will be proportional to the area of surface associated with the nodes.

$$Z_{NS} = Z_{NSO}\ \Delta\theta / \sin\theta\ \Delta\phi \tag{35}$$

$$Z_{EW} = Z_{EWO}\ \sin\theta\ \Delta\phi/\Delta\theta \tag{36}$$

$$Y = Y_o\ R^2 \sin\theta\ \Delta\theta\Delta\phi \tag{37}$$

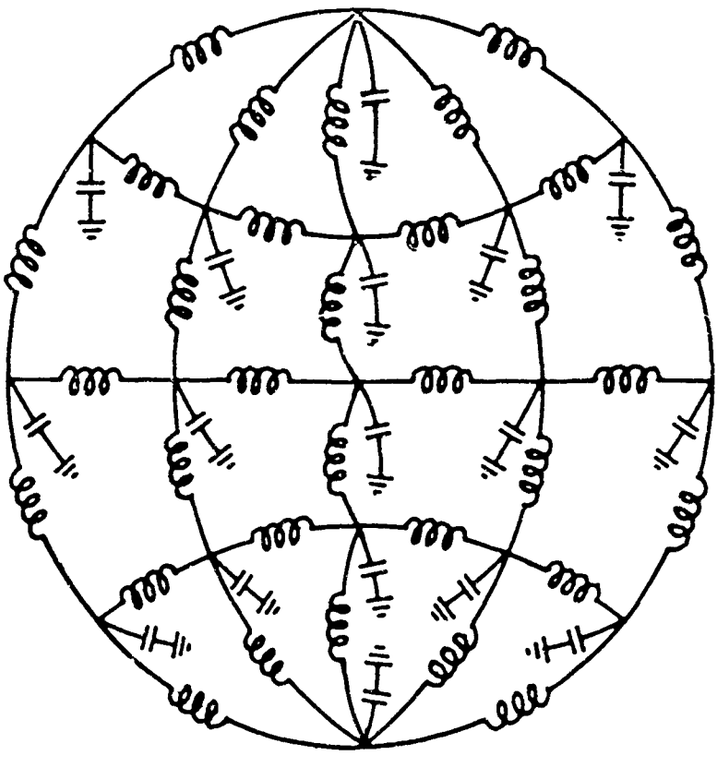

Figure 2 Equivalent circuit for Schumann resonance problem

If the source is at a pole so that we can ignore the ϕ dependence, the network equations, in the limit of an infinite number of nodes, lead directly to the Legendre differential equation.

$$\frac{dV}{d\theta} = -Y_0 R^2 \sin\theta \, \Delta\phi \, I \tag{38}$$

$$\frac{dI}{d\theta} = -Z_0 V / \sin\theta \, \Delta\phi \tag{39}$$

$$\therefore \quad \frac{d^2V}{d\theta^2} = -Y_0 R^2 \cos\theta \, \Delta\phi \, I - Y_0 R^2 \sin\theta \, \Delta\phi \, \frac{dI}{d\theta} \tag{40}$$

$$\therefore \quad \frac{d^2V}{d\theta^2} + \frac{\cos\theta}{\sin\theta} \frac{dV}{d\theta} - Z_0 Y_0 R^2 V = 0 \tag{41}$$

Let $z = \cos\theta$ and since $Z_0 Y_0 = -k_0^2$

$$\frac{d}{dz}\left[(1-z^2)\frac{dV}{dz}\right] + k_0^2 R^2 V = 0 \tag{42}$$

Let $k_0^2 R^2 = \nu(\nu+1)$

$$\frac{d}{dz}\left[(1-z^2)\cdot\frac{dV}{dz}\right] + \nu(\nu+1) V = 0 \tag{43}$$

The resonance condition for this network will occur for $\nu = 1, 2, 3 \ldots$ or $k_0 R = \sqrt{n(n+1)}$ which are the correct resonance conditions for a uniform spherical waveguide. The changing impedances of the network as we approach the poles because of the decreasing area are responsible for setting up partial reflections that modify the waves and cause a phase stagnation around the pole producing a standing wave pattern. This is one way of looking at the behavior of a caustic, but one must remember that this same phase stagnation will occur if the source is placed on the equator, even though now at the caustic, which is on the equator at the opposite side from the source, the impedance values are not changing with position.

To test the accuracy of a lumped-circuit approximation, the resonance frequencies for a circuit with nodes every 10 degrees of latitude were compared with the resonance frequencies of a continuous system. The values obtained are shown in Table IV. In order to make the calculations practical, a small amount of damping was used.

The first three resonant modes are accurate to within 1% or better in the lumped-circuit approximation. Somewhat greater errors can be expected when the source is placed on the equator and a two-dimensional lumped circuit is used. Using a grid of nodes every 10 degrees of latitude and 20 degrees of longitude to represent a homogeneous ionospheric

TABLE IV

Resonance Frequencies of Spherical Waveguide (almost lossless)

Lumped Circuit Approximation Nodes every 10 degrees	True Value	Mode Number
10.58	10.55	1
18.18	18.31	2
25.6	25.9	3
32.6	33.3	4
39.5	40.9	5
46.2	48.4	6

cavity the frequencies of the first three resonant modes were too low by 1, 2, and 3%. A discussion of the error sources is made in the appendix but it is safe to say that the errors will be about the same when the inhomogeneous models are studied. When these circuits are used to study perturbations of the cavity one can expect the changes produced in the resonant frequencies to have the same relative accuracy. Increasing the number of nodes in order to increase the accuracy greatly increases the computational time, but the first order correction obtained by simply increasing the frequencies of the first three modes by 1, 2, and 3% should give ample accuracy for this problem with the $10^{\circ} \times 20^{\circ}$ grid spacing.

IV. GEOPHYSICAL IMPLICATIONS OF THE SCHUMANN RESONANCE DATA

The use of the Schumann resonance data to study phenomena in the ionosphere is still in the early stages, but a few positive results are already beginning to accrue. In this section we wish to examine some of the observational data in the light of the model calculations that were outlined in the previous section, and discuss some of the implications that arise.

The particular points to be examined are the effect of the earth's magnetic field, limits on the lower D or C layer ionization, amplitude and frequency variations of the resonant frequencies, and transient effects of particular ionospheric perturbations.

Magnetic Field Effects

No data at present is available that shows the height dependance of the Schumann resonance signals, although this could be a method of directly measuring the conductivity of the lower D or C regions. It is worthwhile, nevertheless, to examine the theoretical solutions as a function of height, in order to gain physical insight on the wave behavior. The solutions were carried out for a layered model of the atmosphere and ionosphere, and the electromagnetic fields at each layer boundary were computed as well as the fields on the earth's surface. From these results the energy flows could be calculated, and the Q's computed from the rate of energy dissipation. In figures 3 and 4 we show the energy dissipation plotted as a function of height for the mid-latitude daytime

and nightime model. These results follow closely the expected behavior discussed in the second section and re-emphasize the important role played by the earth's magnetic field. The three electromagnetic windows; a radio window in the atmosphere below the ionosphere, a whistler window in the upper D and lower E region, and an Alfven window in the F region and above, are clearly seen. These last two windows are due to the magnetic field. In the daytime model little energy actually reaches the F region, but at night one third of the energy completely escapes the cavity. This results in lower Q's for the nightime propagation even though the phase velocities may be higher. Calculations have been carried out to show that if any of this energy is guided back to the cavity, it produces a negligible effect on the resonance properties.

The magnitudes of the electric and magnetic vectors show different behaviors. The radial electric field is essentially inversly proportional to $\sigma_{rr} - i\epsilon\omega$ and thus rapidly disappears above the effective ionospheric height which is here taken to be where $\sigma_0 = \epsilon\omega$. The horizontal magnetic wave field, however, remains quite constant through this region. The field begins to twist through the whistler mode region and then damps in the transition region. The magnetic field that leaks through this region in the nightime ionosphere suffers very little more damping.

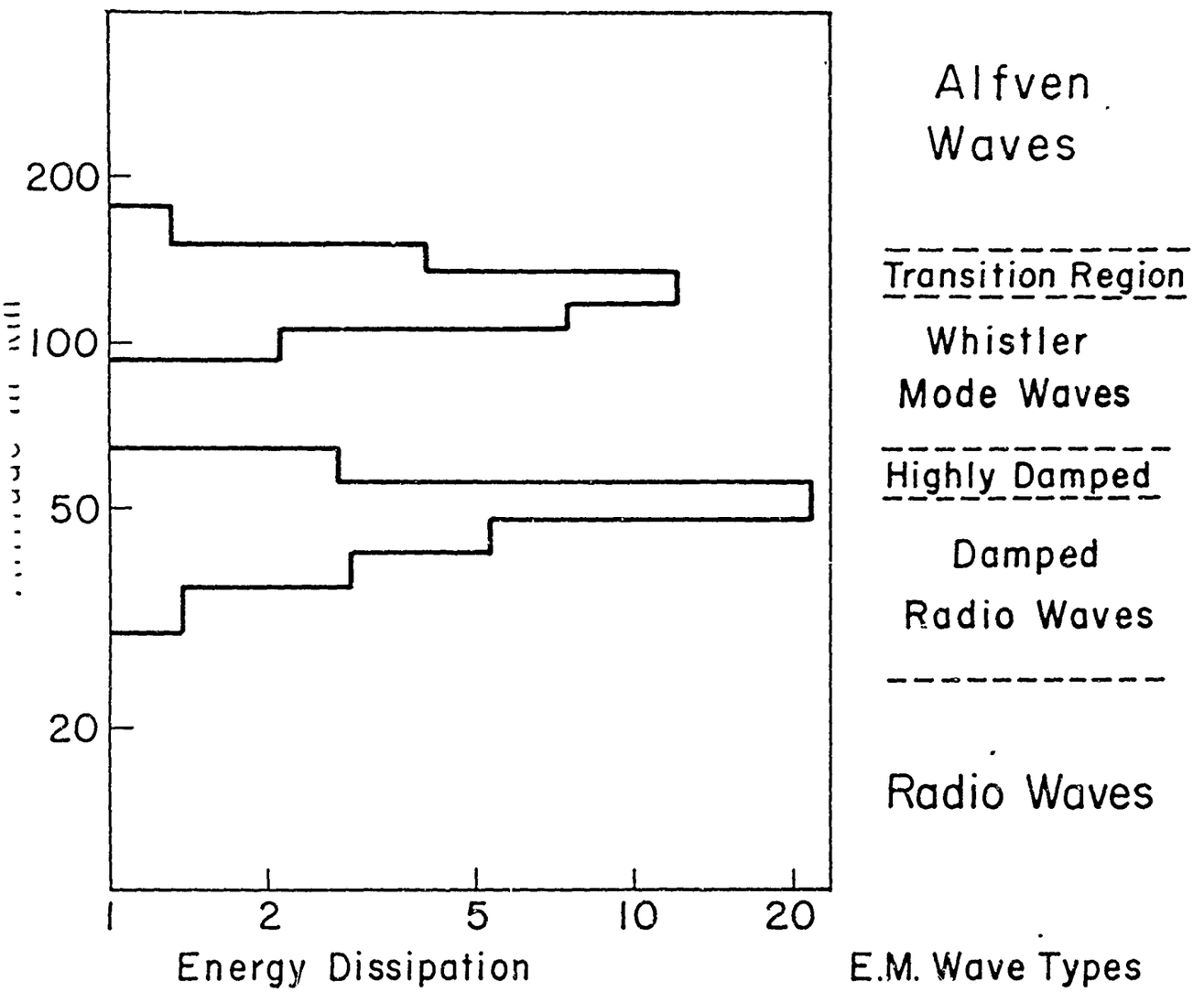

Energy Dissipation and E.M. Wave Types at 7.5 cps
Day-Time Ionosphere Mid - Latitudes

Figure 3 Energy dissipation of Schumann resonances

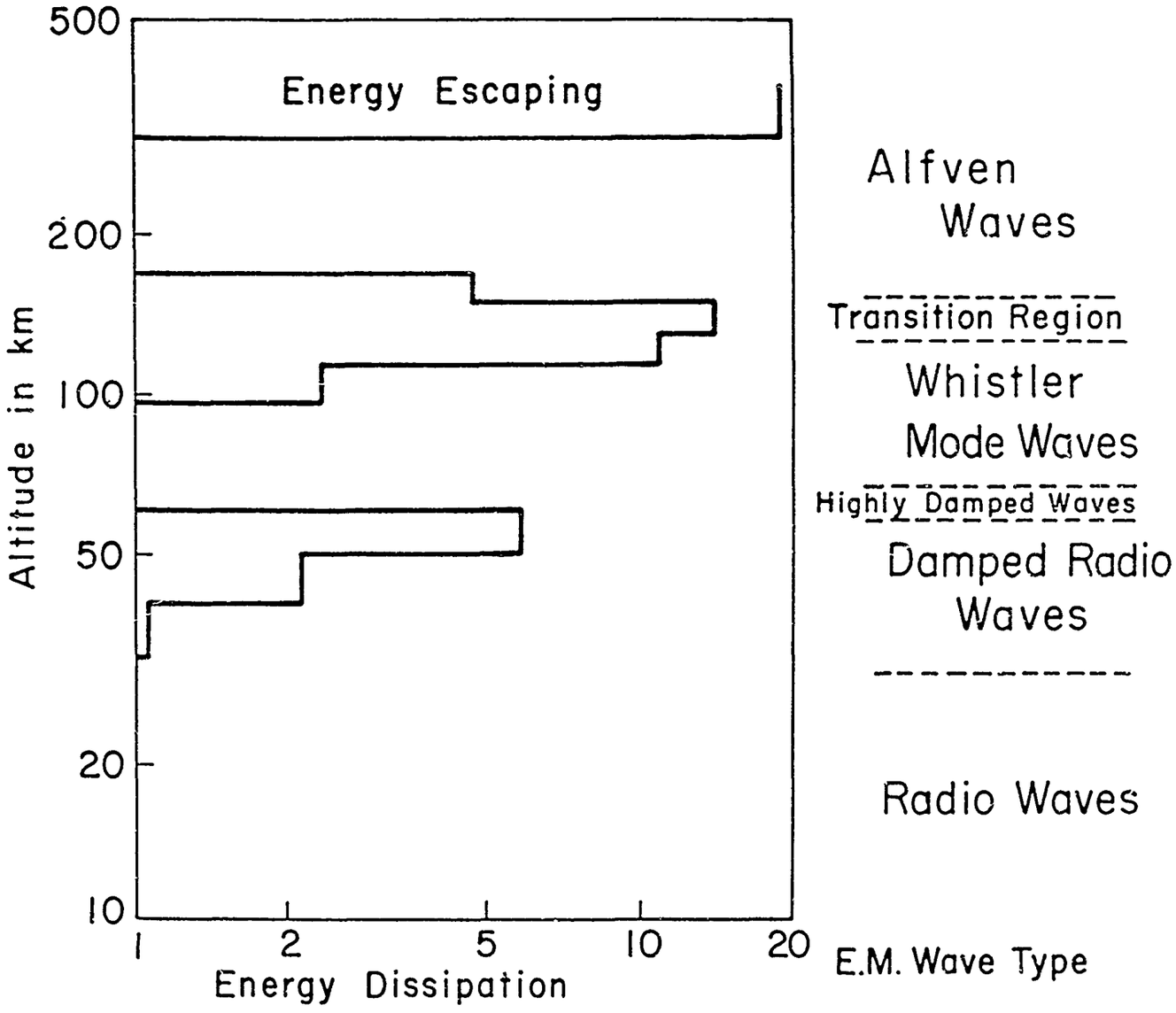

Energy Dissipation and E.M. Wave Types at 7.5 cps
Night-Time Ionosphere Mid-Latitudes

Figure 4 Energy dissipation of Schumann resonances

The importance of the magnetic field is further seen on comparing the solutions derived for different latitude environments. In these computations the ionization levels were the same for the different models, excepting the polar model, but the strength and inclination of the magnetic field simulated the actual field of the earth. Some increase of the C layer ionization which is believed due to cosmic ray ionization was allowed in the polar models. The propagation characteristics of these models are given in Table V. The phase velocities were determined from the phase relationships of the model and are given as a fraction of the velocity of light. The Q's were determined from the ratio of the energy stored to the energy dissipated.

The results of Table V indicate that the magnetic field variations with latitude produce changes in the propagation characteristics that are as great as the day-night variations. The day and night models have different effective heights, however, which will also modify the waveguide impedances.

Some differences of the propagation characteristics were found depending on the direction of the propagation, but these were not very important and Table V represents an average of the N-S and E-W propagation characteristics.

Ionospheric Profiles

The variations apparent in Table V indicate that only crude interpretations of the resonance data can be attempted

TABLE V

LATITUDE DEPENDENCE OF PROPAGATION CHARACTERISTICS

	Daytime Model D11						Nightime Model N12					
Frequencies in cps	7.5		14		20		7.5		14		20	
Latitude	v/c	Q	v/c	Q	v/c	Q	v/c	Q	v/c	Q	v/c	Q
90°	.726	4.77	.759	7.04	.768	8.45	.743	1.46	.741	4.21	.720	3.38
45°	.745	6.00	.766	7.41	.770	9.16	.764	2.73	.720	4.00	.781	3.61
10°	.771	6.76	.784	5.81	.771	11.42	.764	4.00	.761	5.79	.782	5.69
0°	.782	6.97	.801	8.43	.809	9.09	.776	5.85	.804	6.39	.818	6.56

until the full three-dimensional models are worked out. Nevertheless, some modifications of proposed ionospheric models can be made at this stage because of the large discrepancies involved. The Schumann resonance data can most usefully be used to study the very low D regions or the C region because at these low frequencies the conductivity becomes an important parameter in the wave propagation at much lower altitudes than is true for V.L.F. frequencies. Also, since the rocket data is not very dependable at these low latitudes, and the important ionization and recombination reaction rate coefficients are poorly known, the properties of this region are less well determined than those of higher regions of the ionosphere. An example of this state of affairs is shown in figure 5 which gives daytime electron concentration estimates. These estimates include both theoretical determinations based on estimates of the ionization rates and the rates of the modifying reactions, and experimental determinations using ground based and rocket techniques. Most of the recent theoretical work leads to much higher ionization levels than the old ground based determinations as given by Fejer and Gardner (Fejer, 1955; in Gardner, 1954). The more recent experimental data as summarized by Knetch appears to support these higher estimates. (Knetch, 1963.) The theoretical work of Moler and of Arnold and Pierce are exceptions to this trend, however, and their estimates are much more in agreement with the older experimental values. (Moler, 1960; Arnold, 1963.) Much less data, but equally severe discrepancies, are to be

found in the ion concentration estimates. (Bourdeau, 1959; Whipple, 1964.)

It is clear from the results shown in figures 3 and 4 that the ionization levels at around 40-50 KM are very important for the Schumann resonances, and yet we find that estimates of ionization at these levels varying by a factor of 50:1.

The Schumann resonance data must, therefore, be able to discriminate between the two trends shown in figure 5. In figures 6 and 7 are shown the conductivity values, σ_o , that result from these profiles. These estimates also include the ionic contribution. The DWKB model incorporates Whipple's theoretical estimates of electron concentration, Knetbh's summary data on electron concentration and Bourdeau's measurements of ionic conductivity. The same sources are used for the nighttime model NWKB. The D11 model used Moler's estimates of electron concentration and ionic conductivities that are a compromise between Bourdeau's measurements and the measurements reported by Whipple. (Bourdeau, 1959; Whipple, 1964.) The S.I.D. model is based on estimates reported by Nicolet and Aiken (Nicolet, 1960) and by Belrose and Cetiner (Belrose, 1962). The nighttime model N12 also relies on Moler's estimates, and uses the same low level ion concentrations as D11. The collision frequency values used at these levels are essentially those given by Dalgarno (Dalgarno, 1961). This

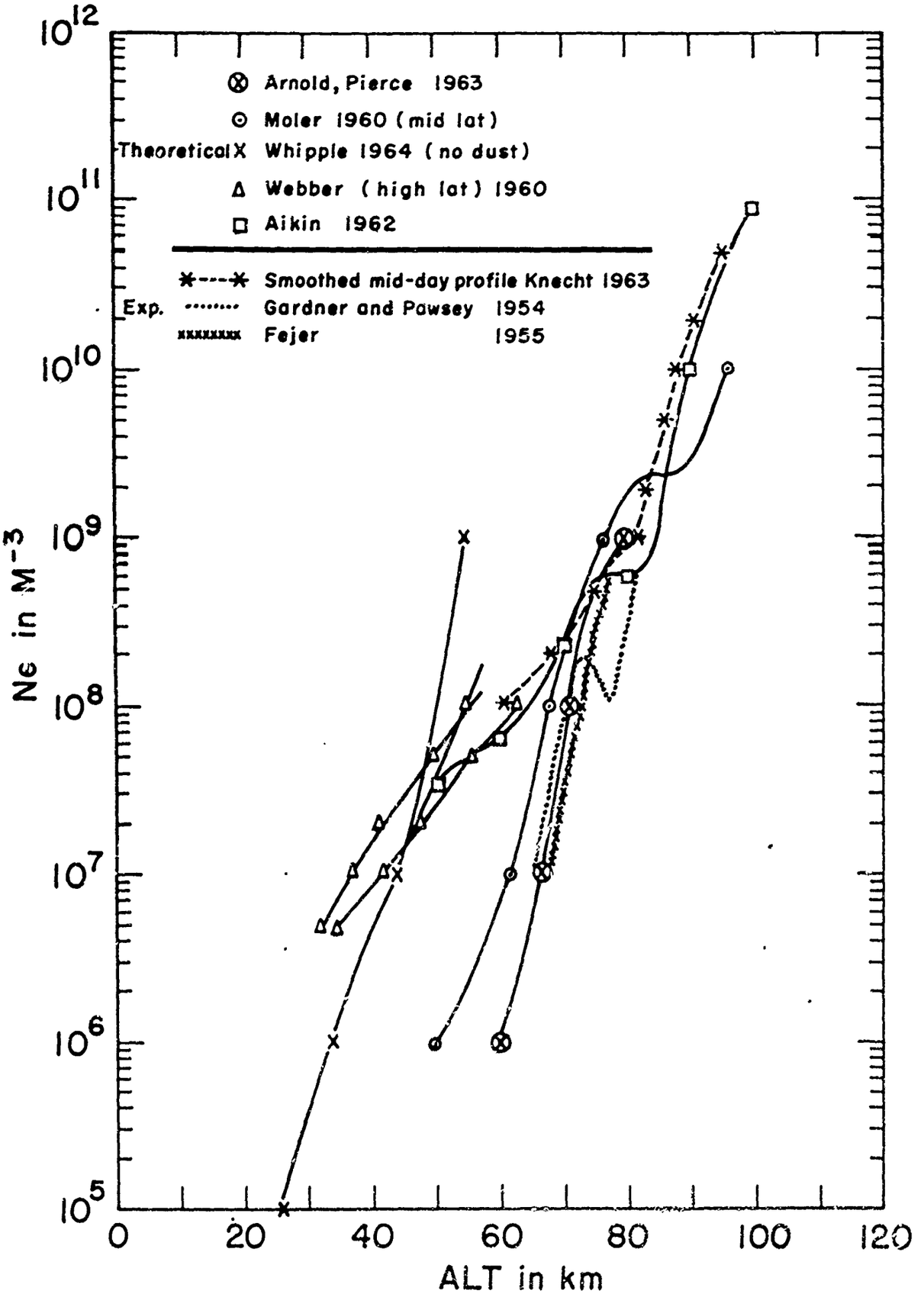

Electron Density Mid-day

Figure 5 Daytime electron density profiles

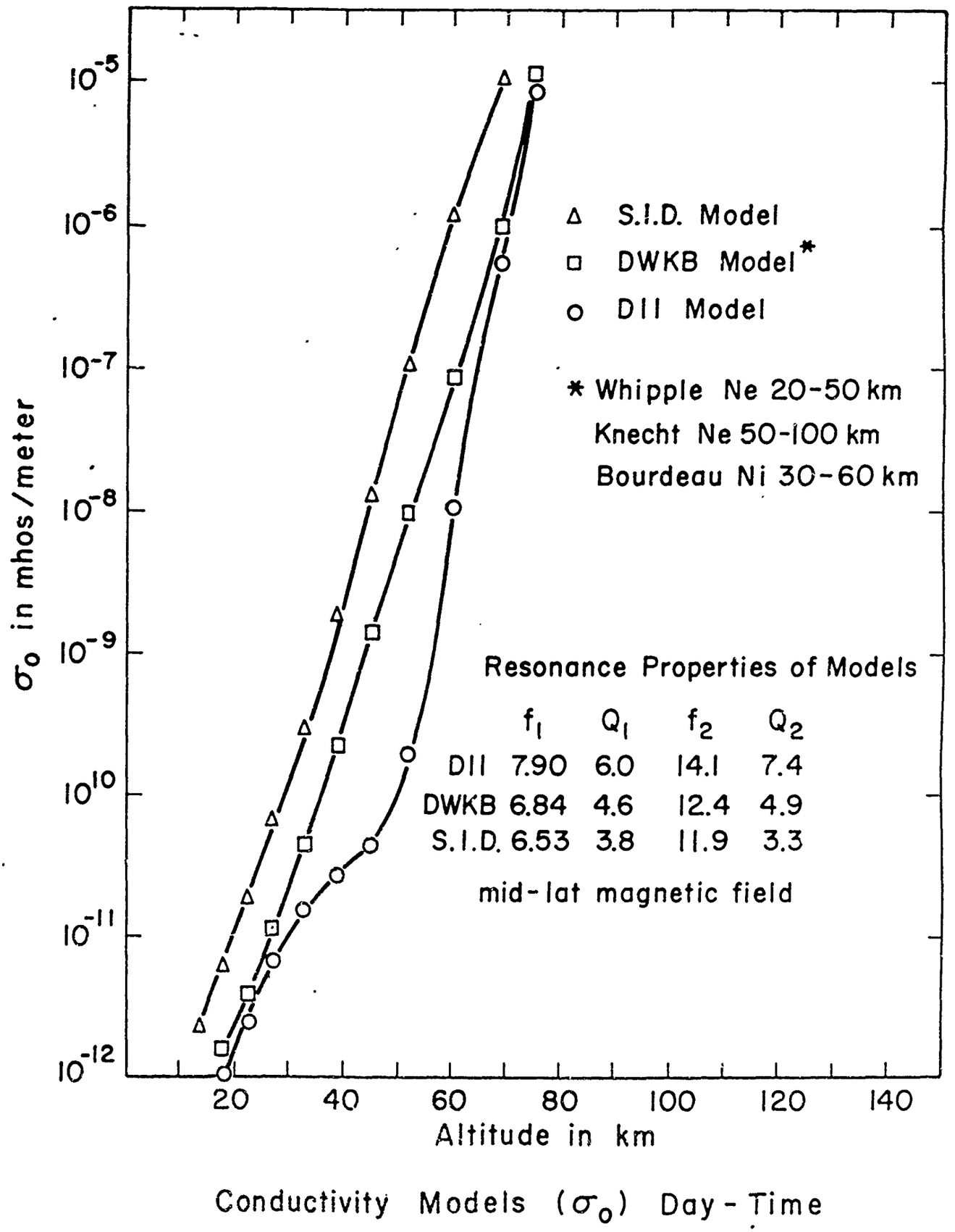

Conductivity Models (σ_o) Day-Time

Figure 6 Daytime conductivity models and resonance properties

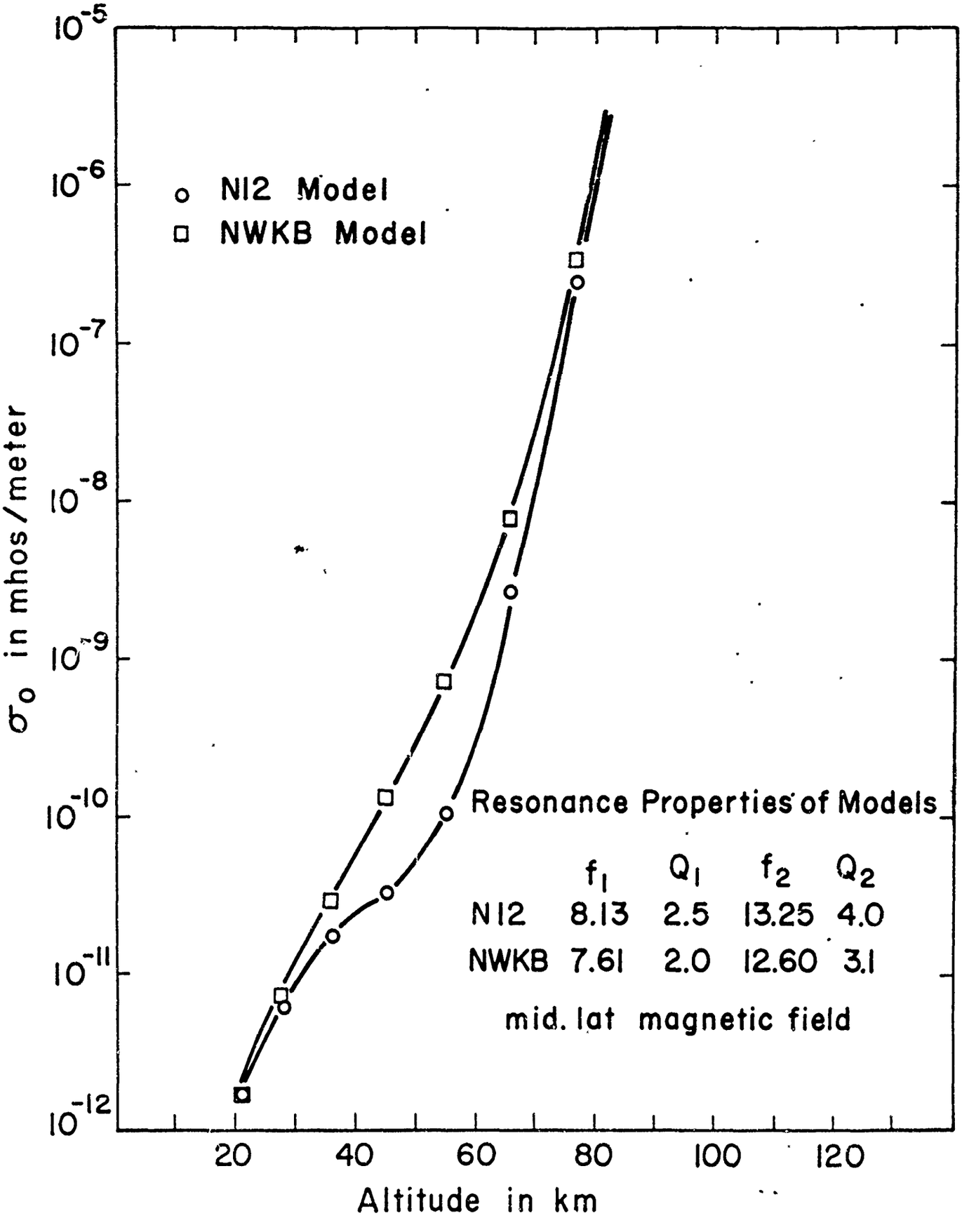

Conductivity Models (σ_o) Night-Time

Figure 7 Nightime conductivity models and resonance properties

data is summarized in Table VI.

The resonance properties that are also given in figures 6 and 7 are based on the ionospheric models being uniformly distributed over all the earth's surface, and are therefore not realistic, but still the results clearly discriminate against the DWKB and NWKB models. The phase velocities and Q's of these models are so low compared to the data obtained from the Schumann resonances that one must reject these models as providing too much ionization. Whipple discusses the possibility that his estimates are too high and suggests that dust particles are responsible for sweeping up much of this low level ionization. It seems unlikely that the dust levels are high enough to accomplish this much of a change, and if so the Schumann resonance data should be very sensitive to influxes of dust such as result from the meteor showers, for which there seems to be no evidence. It is more likely that the reaction rate constants that are important in the theory tend towards the values used by Moler.

The more complete calculations using the D11 and N12 models for the day and nightime ionization levels gave very reasonable results and most of the calculations to be discussed in the rest of this section used these models.

TABLE VI

PARAMETERS OF IONOSPHERIC MODELS

H	D_{11} Ni	D_{11} Ne	N_{12} Ni	N_{12} Ne	νin	D11 (νei + νen)	N12	MW
0	6×10^{8}		6×10^{8}		1.1×10^{10}			29
30	1.4×10^{9}		1.4×10^{9}		1.5×10^{8}			29
40	1.3×10^{8}	2×10^{5}	1.3×10^{8}		3.5×10^{7}	3.4×10^{8}	3.4×10^{8}	29
50	5.6×10^{8}	1×10^{6}	5.6×10^{8}	2×10^{4}	1×10^{7}	1.0×10^{8}	1.0×10^{7}	29
60	3×10^{8}	1.1×10^{7}	3×10^{8}	2.5×10^{5}	1.5×10^{6}	2.9×10^{7}	2.9×10^{6}	29
70	2×10^{8}	1.8×10^{8}	2×10^{8}	2.5×10^{6}	3.5×10^{5}	5.4×10^{6}	5.4×10^{6}	29
90	1×10^{10}		3×10^{8}		1.6×10^{4}	4.0×10^{5}	2.4×10^{5}	29
100	5×10^{10}		2.5×10^{9}		3×10^{3}	1×10^{5}	4.5×10^{4}	28
150	3×10^{11}		3×10^{9}		3×10^{1}	3×10^{3}	4×10^{2}	24
200			3.5×10^{9}		4×10^{0}		1.0×10^{2}	21
250	1×10^{12}				1.5×10^{0}	1×10^{3}		19
270			4×10^{9}		1×10^{0}		6.0×10^{1}	19
300			1.2×10^{11}		6×10^{-1}		2.0×10^{2}	18
380			2.5×10^{11}		1.5×10^{-1}		2.5×10^{2}	17

H in Km

N in M^{-3}

in sec^{-1}

In order to test the sensitivity of the Schumann resonances to changes of these ionization levels, the resonance properties of slightly perturbed models were also computed. These results are given in Table VII. Ionization increases in the C and lower D regions always reduce the resonant frequencies and the Q's, but the effect is less pronounced at the higher frequencies. Ionization increases at higher levels produce more complex effects. In the day time increases of the E layer ionization increases the frequency and Q of the first mode, but decreases the frequency and Q of the third mode. At night the Q's were increased for all of the first three modes when the E layer ionization increased, but the Q of the first mode was decreased and the Q of the third mode increased when the F layer ionization increased. It would be very difficult to interpret the E and F layer variations from observations of the Schumann resonances, but there are many other techniques for observing these layers. The Schumann resonances are most sensitive to changes of the D and C regions and the use of the resonance data will probably be confined to studying these regions of the ionosphere.

Diurnal Variations

The diurnal variations of the background E.L.F. noise power are perhaps the best documented features of the Schumann resonance phenomenon. (Holzer, 1956, 1958; Aarons, 1956; Raemer, 1961; Balser, 1962; Polk, 1962; Stefant, 1963.) The first investigators realized that the

TABLE VII

EFFECT OF IONOSPHERIC PROFILE PERTURBATIONS ON SCHUMANN RESONANCE PROPERTIES

Mid Latitude Magnetic Field

Model	f_1	Q_1	f_2	Q_2	f_3	Q_3	Perturbation of Ne and N1 Height in KM	30	50	70	90	100	150	200	270	300
D11	7.90	6.0	14.10	7.4	20.0	9.2										
D11P	7.72	4.7	14.0	5.7	19.9	7.6		x2	x2	x2						
D11UE	8.00	7.3	14.03	7.2	19.35	6.2				x1.5	x3	x4	x3			
N12	8.13	2.5	13.25	4.0	20.3	3.6										
N12P	7.70	2.2	12.6	3.3	19.7	3.2		x2	x2	x2						
N12UE	7.77	5.4	14.2	6.1	19.8	6.2					x3	x4	x3			
N12UP	7.67	1.9	13.4	3.0	19.7	5.4								x3	x25	x8

general activity was related to the world wide thunder storm activity. The ratio of the amplitudes of the various modes is mainly determined by the location of the receiver relative to the nodes of the standing wave patterns set up by the source. This is modified by the source spectrum and by the complications of an inhomogeneous wave guide, and by the frequency dependence of the damping factors. Raemer attempted to adjust the source distributions in order to explain the observed spectra, but because of still unresolved factors concerning the wave propagation complications and the source spectra, these results are somewhat qualitative. Nevertheless the general agreement with the known thunderstorm areas is good enough to warrant some confidence in our general understanding of the sources of the observed resonances. Similar, but more qualitative, results have been reported by other investigators (Holzer, 1958; Balser, 1962; Rycroft, 1963, Stefant, 1963). During the Northern Hemisphere winter the main areas of thunderstorm activity occur on the equatorial land areas at around 16:00 local time. During the summer important sources also develop in the mid-latitude continental regions of the Northern Hemisphere (Handbook of Geophysics, 1960). Figure 8 shows the diurnal power variations that would be predicted for a localized source occurring at 16:00 local time on the equator recorded in New England. Some recent winter time data for New England provided by Balser and Wagner is also shown. The general features of the observed data could be explained by

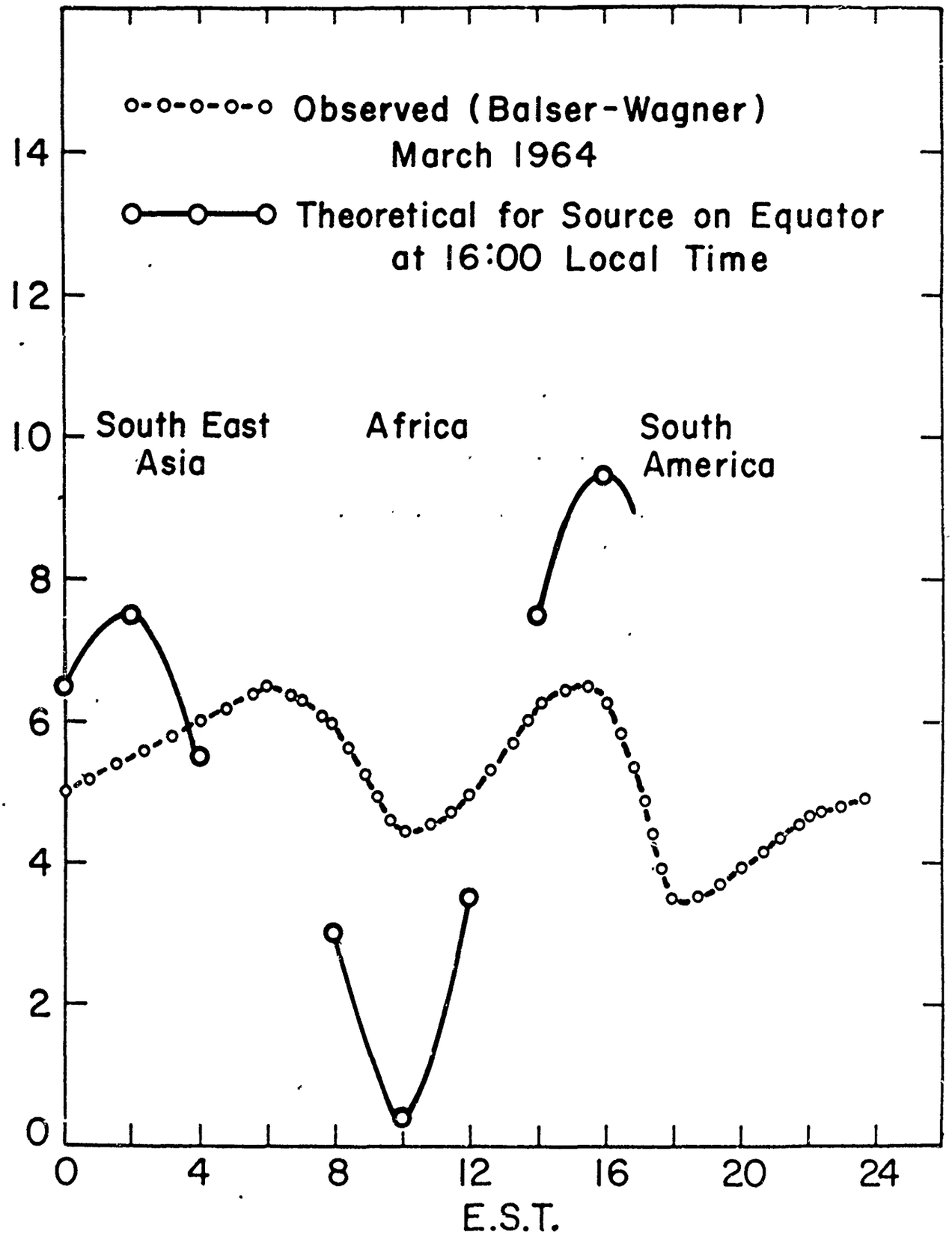

Diurnal Power Variations 1st Mode

Figure 8 Theoretical and observed diurnal power variations of first resonant mode for New England

increasing the importance of the African sources and including a background of more scattered sources. In these solutions it should be pointed out that not only are the variations of the waveguide propagation constant brought into play, but also the impedance changes of the waveguide. A most important parameter in determining the impedance is the effective ionospheric height, Alt. The ionospheric height plays a further role when the amplitudes of the vertical electric field are being considered, since in the transmission line analogy E_z is equated not to V , but to V/Alt.

Added information can be provided by examining the power in the various components of the magnetic variations produced by the Schumann resonances. Unfortunately, some of the reported magnetic data has not specified the components involved.

In order to make more quantitative use of the power level data one should really have data from a network of stations distributed over the entire earth.

While there is a good general understanding of the reasons for the observed diurnal power variations, little work had been done to explain the observed diurnal variations of the apparent resonant frequencies. Systematic studies of these variations have only been reported by Balser and Wagner (Balser, 1962), but some examples of these variations

are also given by Stefant (Stefant, 1963). These observers have all noted that the variations were not systematic among the various modes and therefore were not primarily due to systematic variations of the ionosphere. Balser has suggested that the variations are due to the interplay of the various harmonic modes as the source receiver geometry is changed. As was discussed in the last section, the wave field in a spherically symetric waveguide can be described in terms of a set of spherical harmonics, $P_n(\cos\theta)$. The magnitude of each term in the harmonic series depends on how close the excitation frequency is to the resonant frequency for that harmonic, and the Q. When the Q is high and the excitation frequency is equal to a resonant frequency the amplitude of that harmonic is so large the other terms can be ignored. In such a case one would observe a peak in the power spectrum at this resonant frequency for a broad frequency source almost everywhere except at the nodes of the harmonic function. As the Q becomes lower the other terms in the harmonic series become important further away from the node zones, and also the shape of the source frequency spectrum can begin to alter the observed peak frequencies. Also as asymetries are brought into the waveguide system, the harmonic series must be expanded, each term splitting into 2n + 1 terms, $P_n(\cos\theta) \rightarrow P_n^m(\cos\theta)$, $m = -n, -(n-1) \cdots n$. When the asymmetry is small the frequencies associated with the m values for a given n value are close together, and the effect is known as line splitting. In such a case even higher values of Q

are necessary in order for the resonant frequency to excite only one harmonic mode. With the modest Q values that we find in the Schumann resonances the resonant frequencies must excite quite a bit of energy in many other harmonic modes and the line splitting, though present, will be masked. As the receiver moves around relative to the source the ratio of the amplitudes of the excited modes change and these changes modify the observed spectrum.

Another way of describing this situation is shown in figure 9. Here we show the power levels for two frequencies near the resonant frequency. It is noticed that the node zones move as the frequency varies. This would not be possible if only one harmonic mode was involved. It is readily apparent that the ratio of the power of these two frequencies varies with position, so that the power spectrum shape will also vary. The resulting variations of the apparent resonant frequency are shown in figure 10 for two different Q values. Although the computations in figure 10 were done for a uniform waveguide model the changes in the apparent resonant frequency for the Q of 5 are comparable in magnitude to the observed diurnal variations. When the more realistic D11 - N12 model is used the predicted apparent resonant frequencies and their diurnal variations are in close agreement with the observations as is shown in figure 11. Again the agreement would be improved if the localized

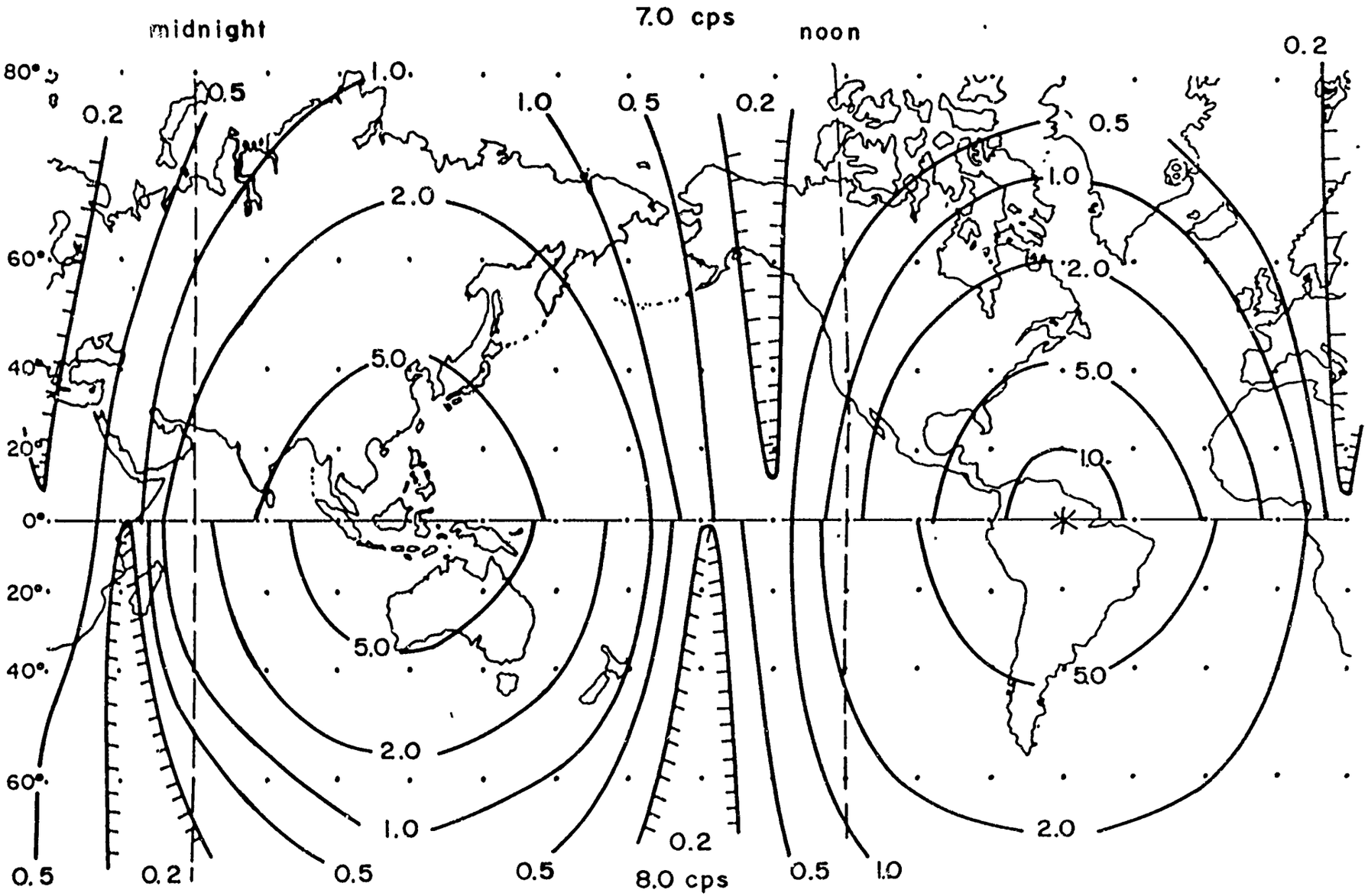

D3-N3 Model Power Density 20.00 GMT

Figure 9 Power density variations for neighboring frequencies

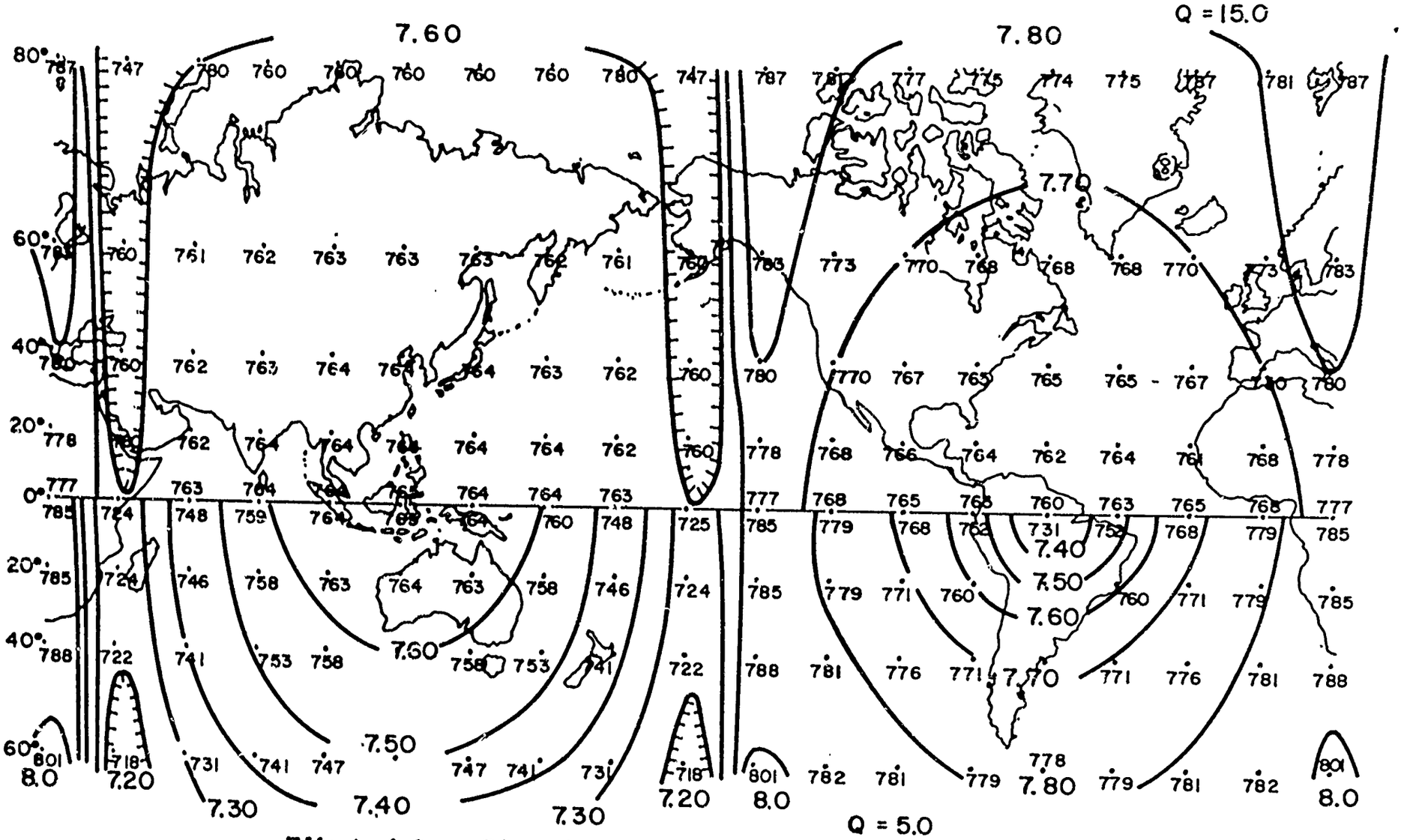

Effect of Q on Diurnal Frequency Variations of First Mode Apparent Resonant Frequency with Source in South America Uniform Ionospheric Model

Figure 10 Apparent resonant frequency variations for different Q values

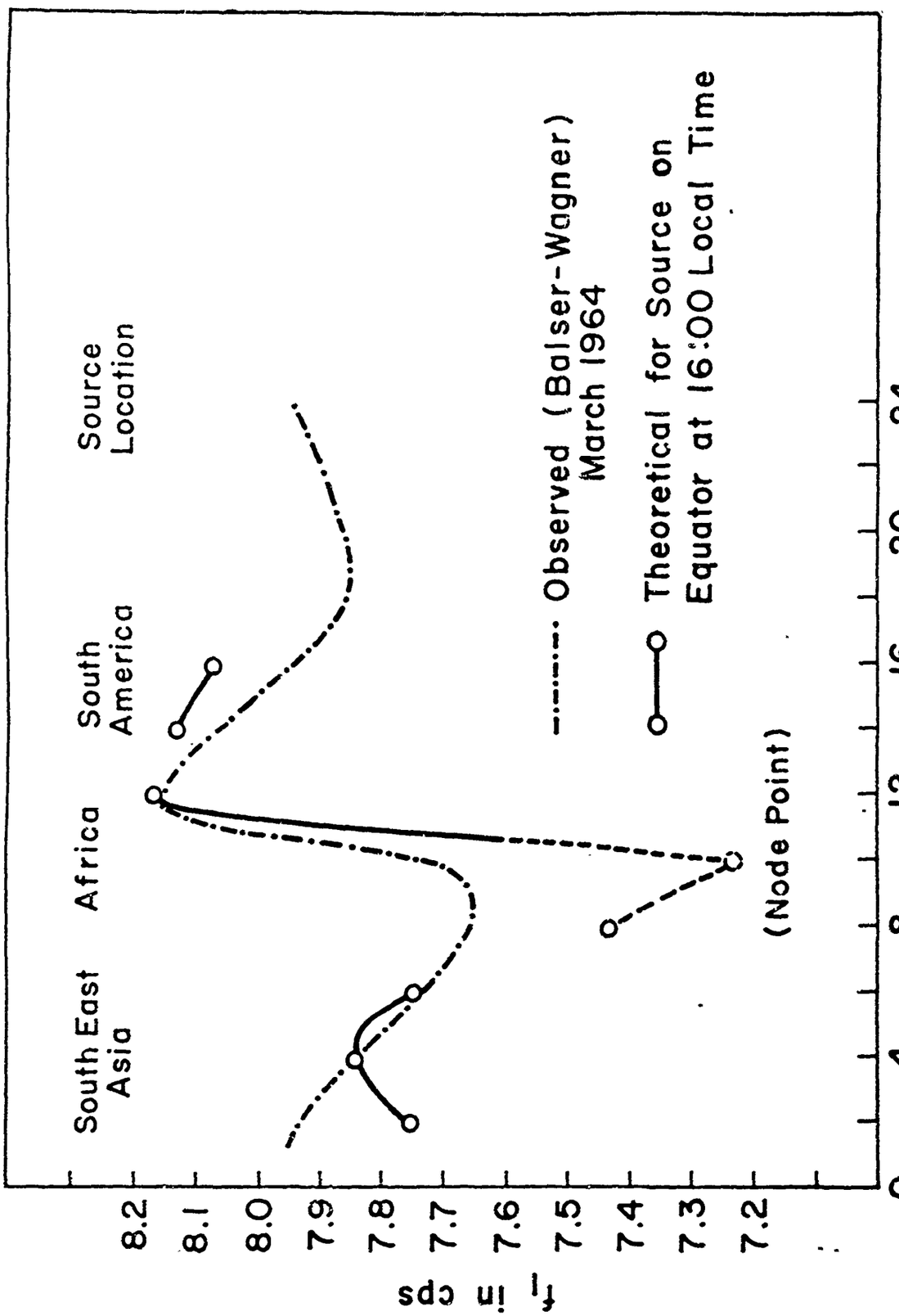

Figure 11 Diurnal Frequency Variations of f_1

source was augmented by a background of more widely scattered sources. It appears, however, that the essential features of the diurnal variations are explained by the mode mixing, and no particular systematic variations of the ionosphere are needed, in agreement with Balser's suggestion.

Since the shape of the power spectrum is used to compute an apparent Q as well as the apparent resonant frequency, the observed Q's should also show a diurnal variation. A summary of the predicted results from the D11 - N12 model is given in Table VIII. The two dimensional model used to calculate these results used the propagation characteristics given in Table V, as well as the appropriate effective ionospheric heights and interpolated those values as a function of latitude, longitude, and frequency. The longitude dependance was assumed constant except for a 20 degree strip connecting the day and night ionospheres. The Southern and Northern hemispheres were assumed to be symetric so that the tilt of the earth's magnetic axis was ignored, as well as any north-south assymetries produced by the tilt of the earth's axis of rotation from the ecliptic.

Transient Variations

Perhaps some of the most interesting applications of the Schumann resonance studies are their use in tracking large scale ionospheric perturbations associated with special events. The only well documented example is the effect of

TABLE VIII

APPARENT RESONANT FREQUENCIES AND Q's OF D11-N12 MODEL EQUATORIAL SOURCE AT 16:00 LOCAL TIME

Receiver at 20° latitude

t_1*	f_1	Q_1	t_2*	f_2	Q_2	t_3*	f_3	Q_3
04:00	8.04	3.9	04:00	14.1	5.2	00:00	20.2	4.8
16:00	7.80	4.1	10:40	13.7	5.6	04:00	19.7	4.7
			16:00	14.0	6.5	08:00	20.0	5.2
			21:20	13.7	5.5	12:00	19.8	7.3
						16:00	20.2	5.2
						20:00	19.9	6.4

Receiver at 40° latitude

04:00	7.96	3.6	04:00	13.7	5.2	00:00	19.8	5.3
16:00	8.07	6.0	10:40	14.0	5.5	08:00	19.7	6.1
			16:00	14.4	10	12:00	20.1	5.8
			21:20	13.8	5.4			

Receiver at 60° latitude

04:00	7.72	3.5	04:00	14.7	8.3	01:20	19.7	5.2
16:00	8.14	8.5	10:40	14.0	5.4	05:20	19.8	4.3
			21:20	14.0	5.3	14:40	19.8	5.8
						18:40	20.1	4.9

* The t's represent local times of energy maxima

the Starfish high altitude nuclear explosion of July 9, 1962 (Balser, 1963; Gendrin, 1962). It appears that a systematic change of the resonance properties occurred immediately following the explosion over Johnston Island, and the resonant frequencies of the first four modes were decreased by .55, .55, .9 and .9 cps (Stefant, 1963), as observed in France. The effect decayed away in a period of hours. A similar decrease of the first mode was observed in New England (Balser, 1963). The time resolution of the effect is of course not sharp since it takes several minutes to get a statistically significant determination of the resonant frequencies. Since the resonance properties represent a world wide averaging of the waveguide parameters, it is clear that these anomalies must have been caused by a very extensive perturbation of the ionosphere. It now appears, from radio propagation studies made in Japan and in the United States, that the entire Pacific area was immediately heavily ionized to low altitudes by the explosion. (Maeda, 1964; Zmuda, 1963) These results, as we shall see, are substantiated by the Schumann resonance data. This ionization occurred within the first second of the explosion. The time resolution of the measurements do not allow much closer definition, and it is still not clear what were the primary sources of this ionization. Some of the initial ionization may have been fast gamma irradiation. If this were the case the sources of the gamma radiation must have been shot up far above the explosion site since radio and optical effects were observed in the western part of the United States (Odencrantz, 1962; Zmuda, 1963; Moler, 1964).

Other sources of ionization were probably supplied by the neutron decay products. Studies of the geometry of this radiation indicate that the entire Pacific would be involved (Kenney, 1963; Oelbermann, 1964). Further ionization resulted from the dumping of energetic particles that were put into trapped orbits by the explosion (Zmuda, 1963). A more localized, but longer lasting, source of ionization would be the decay of fission products (Williams, 1962).

The Schumann data is not suited to tracking the rapid sequence of events that followed the explosion, but it does throw some light on the geometry of the ionization. In order to study this problem we first considered as a perturbation model heavy ionization in an area of about 6000 km by 8000 km, centered over Johnston Island in the night side. The ionization model used was similar to the ionization levels that occur in the artic regions during PCA events. If such ionization occurred uniformly over the entire earth the first mode would be lowered to 5.7 cps, but when the zone was restricted to 48×10^6 square kilometers around Johnston Island the lowering of the first mode resonant frequency was only .05 cps. In figure 12 we show the phase changes that this perturbation would cause at 7.5 cps for a source located just south of India. There is some distortion of the phase contours, but over most of the earth's surface the phases are hardly changed. Such a map, of course, could not be drawn up from direct observations of the Schumann resonances, since the actual sources are random.

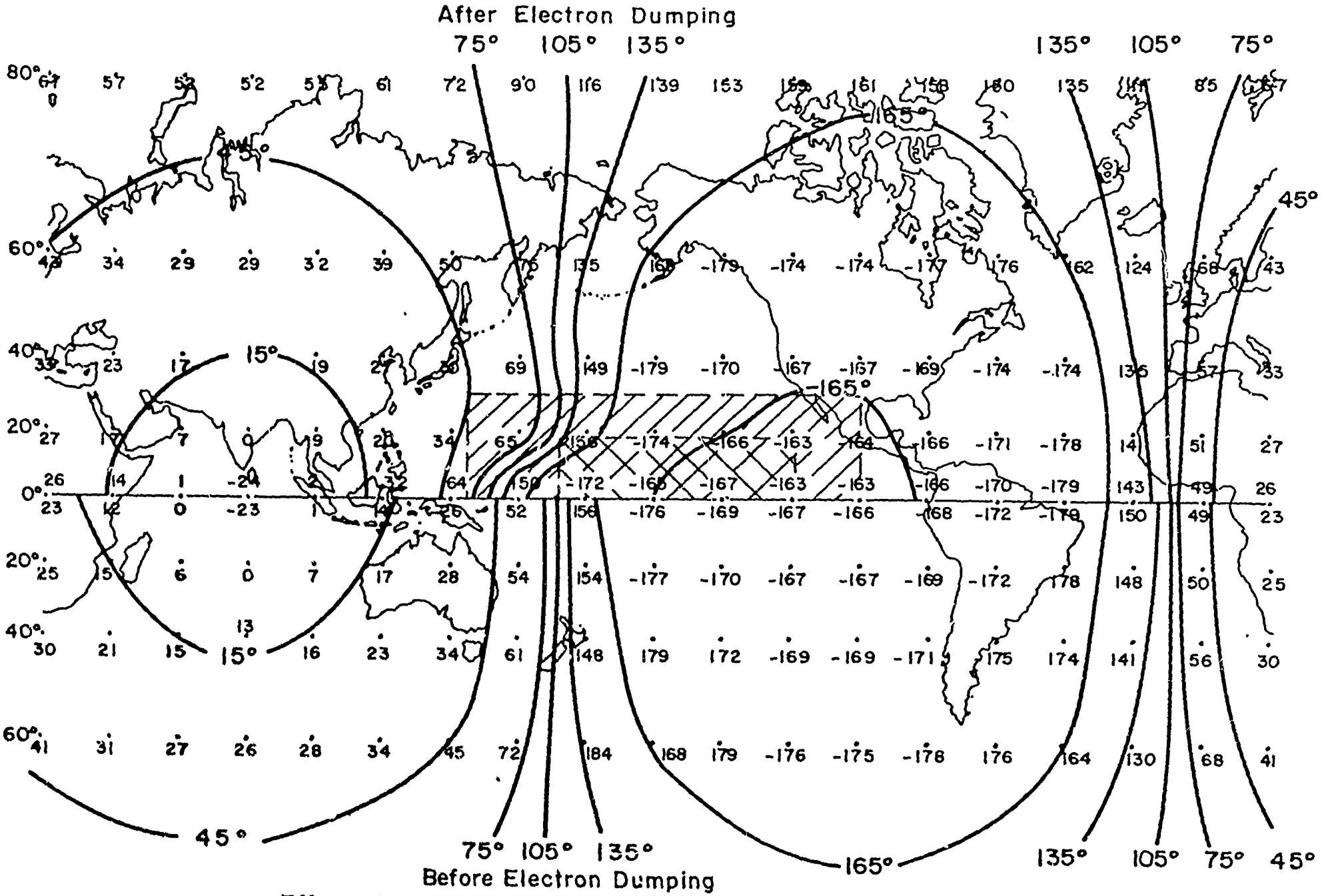

Effect of Electron Dumping on Equatorial Midnight Zone
Phase Contours at 7.5 cps

Figure 12 Phase changes produced by heavy ionization over Johnston Island

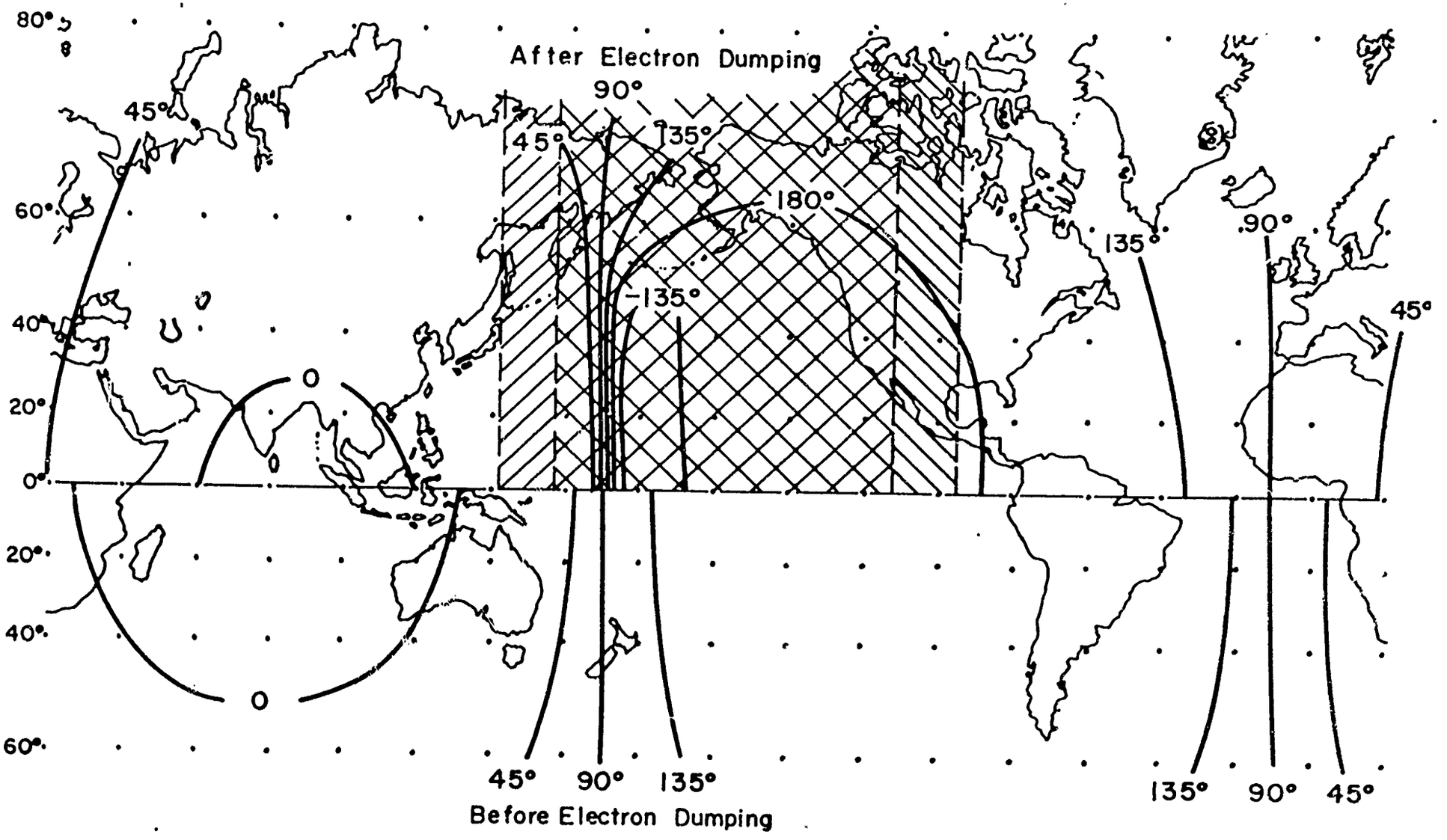

Effect of Electron Dumping on Midnight Third of DII-NI2 Model
10:00 G.M.T. Phase Disturbance at 7.5 cps

Figure 13 Phase changes produced by heavy ionization over the entire Pacific

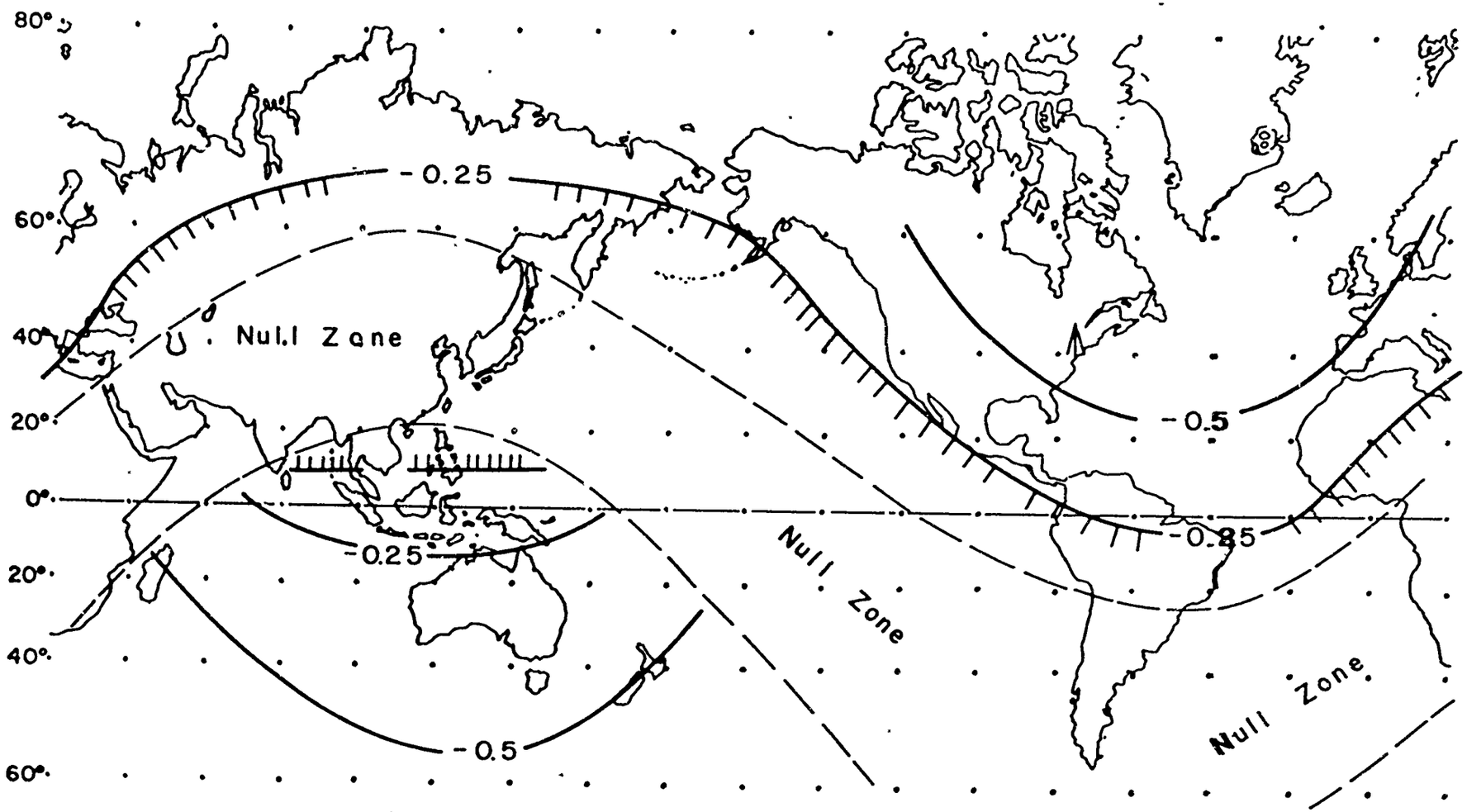

Effect of Electron Dumping on Midnight Third of DII-NI2 Model
Responce Function of Receiver in Northeastern U.S.A.
10:00 GMT Frequency Shift of Apparent Resonant Frequency 1st Mode

Figure 14 Effect of Starfish ionization model on Schumann resonances observed in New England plotted as a function of the source location

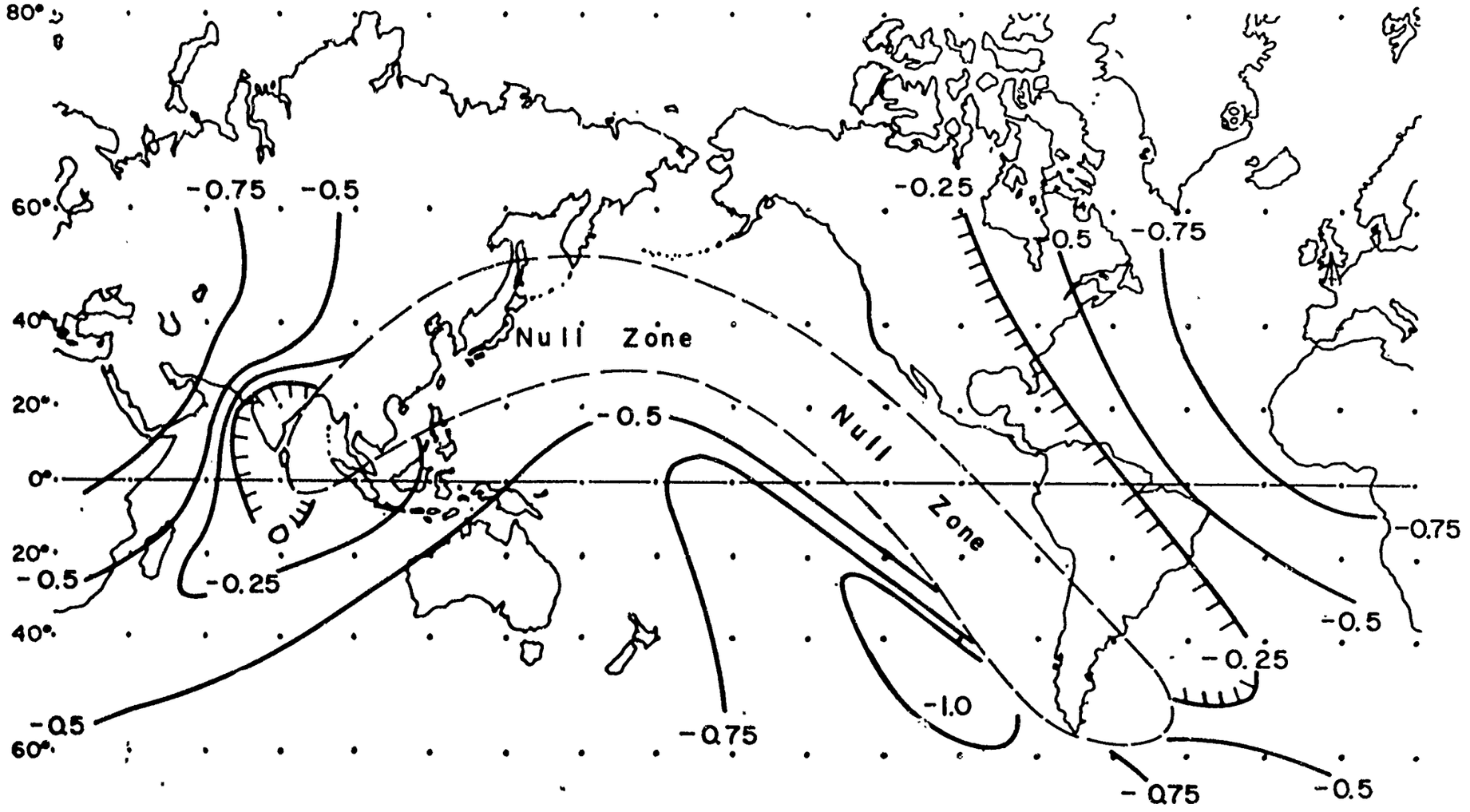

Effect of Electron Dumping on Midnight Third of DII-NI2 Model
Responce Function of Receiver in Western France
10:00 GMT Frequency Shift of Apparent Resonant Frequency 1st Mode

Figure 15 Effect of Starfish ionization model on Schumann resonances observed in France plotted as a function of the source location

It is evident from these results that the ionization effects of the Starfish explosion were far more extensive in area than the model used in figure 12. As a second model we considered a less intense ionization equivalent to the S.I.D. model of figure 5, but spread out over the entire Pacific area and covering about one third of the earth's surface. The phase changes of this model are shown in figure 13. This model does produce effects large enough to be compared to the actual effects of July 9. It should be noted in figure 13 that the caustic which is marked by the large area of almost constant phase disappears because of the severe assymetry introduced by the bomb perturbation.

In order to compare the effect of this model with the observations made in France and in New England we must also consider the source locations, since the apparent resonant frequencies vary with the latter. Therefore, in figures 14 and 15 we plot the resonant frequency shifts of the first mode that would be observed in New England and in France as a function of the source location. If the major lightning sources at the time were located in Australia the observations in France would be predicted, but the observations in New England would be not quite predicted. Additional sources located in central and northern North America might have improved the fit, but it certainly seems that the ionization model used is neither too extensive nor too severe. The areas that are marked null zones represent areas that are

nodes relative to the receiving site. One cannot really carry this study much further without a better knowledge of the source locations, and a wider distribution of observing sites.

It is also possible to study the effects that are to be expected from some of the naturally occurring ionospheric perturbations. In figure 16 we plot the predicted effect of an S.I.D. The ionization model was the same one used to model the Starfish effect, but the perturbation occurred on the daylight side not the night side. In figure 16 the apparent resonant frequency shift is plotted as a function of the receiver location for a source at 16:00 local time, which is depicted as in eastern South America. The general level of the effect is comparable to the Starfish effect.

In figure 17 we show the predicted effect of a P.C.A. event. The ionization perturbation used is more intense than the S.I.D. model, but, since the effect is confined to the auroral zones, a much smaller area is involved and the Schumann resonances are less effected. Not only are the magnitudes of the two effects different, but also the pattern of the effects are quite dissimilar. It appears that one might be able to interpret the geometry of the ionospheric perturbations from a knowledge of the pattern of the Schumann resonance perturbations. At present there does not seem to exist enough data to undertake such

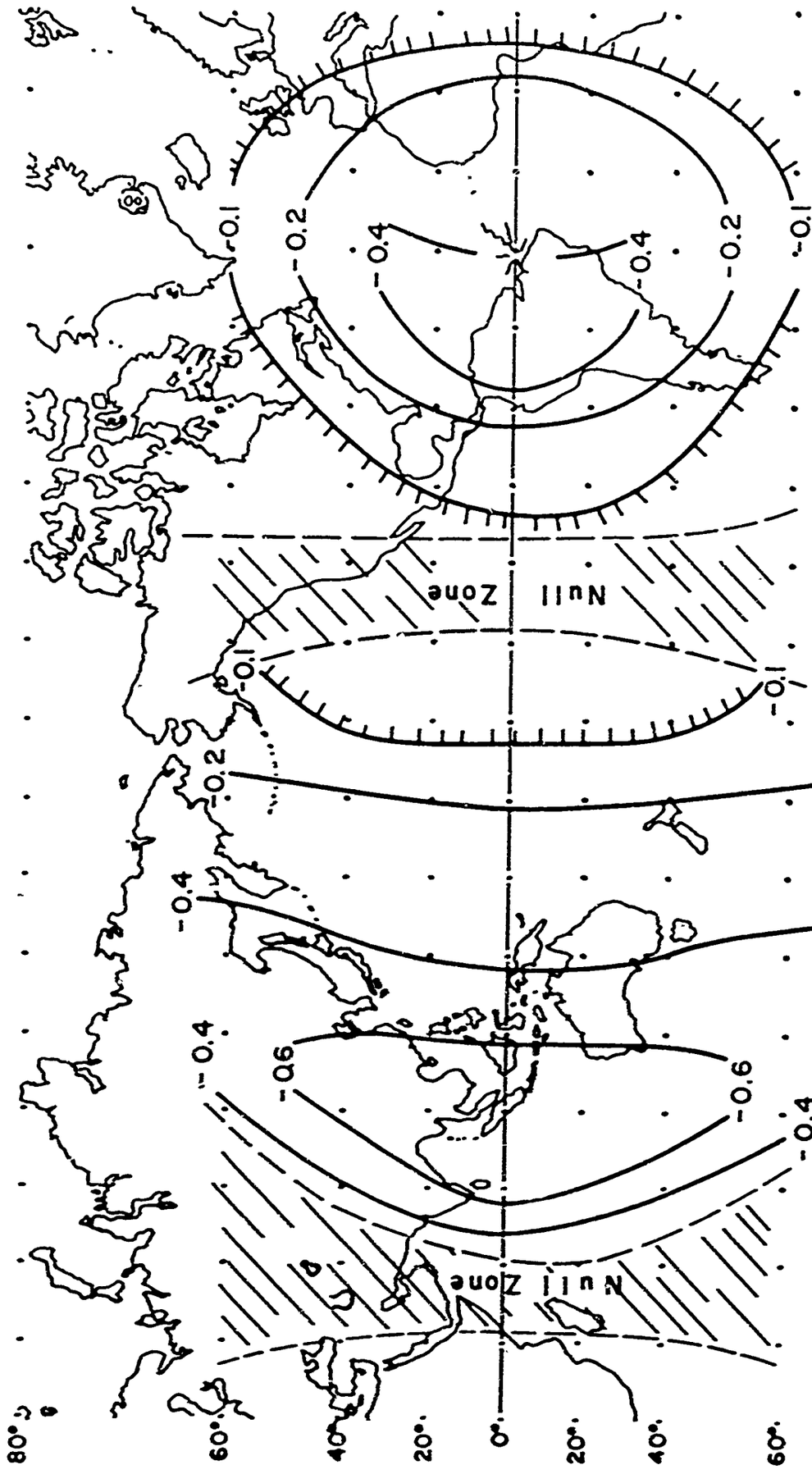

Figure 16 Predicted Schumann resonance perturbations due to an SID event plotted as a function of receiver location

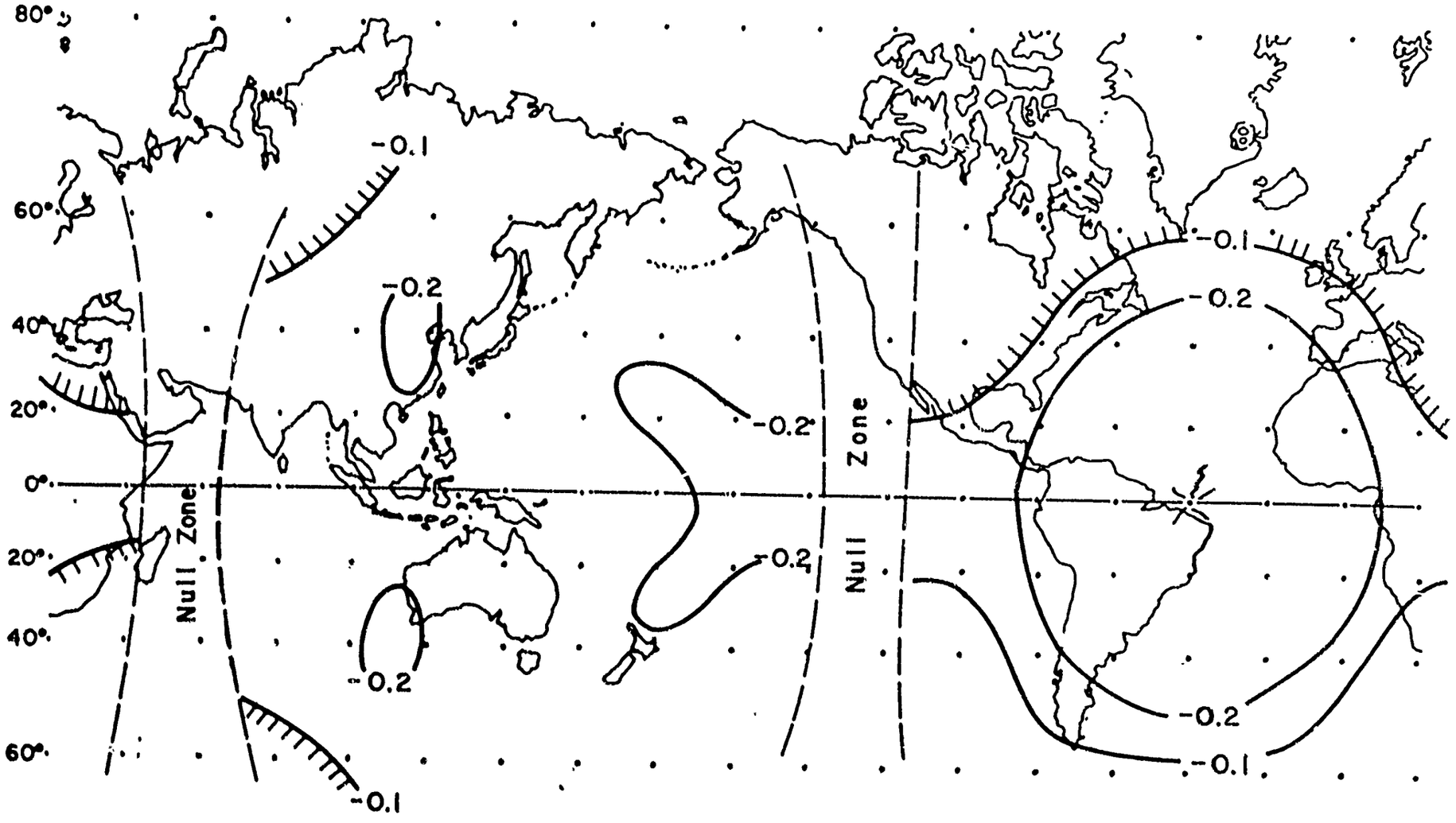

Effect of P.C. A. Event on DII-NI2 Model
19:00 GMT Frequency Shift of Apparent Resonant Frequency 1st Mode
Source Function for Lighting in Brazil

Figure 17 Predicted Schumann resonance perturbations due to a PCA event plotted as a function of receiver location

a study. The only recorded study of such a naturally occurring perturbation was by Chapman and Jones (Chapman, 1964) who reported a substantial increase of the first mode frequency associated with a P.C.A. event. This would seem somewhat unlikely, but warrants further study.

Additional information can be obtained from the amplitude of the resonance signals. Unlike the frequency values, the amplitude values can be influenced by local perturbations directly over the receiver or the source. This can be a disadvantage for some studies, but an advantage for other studies. An interesting application of this local effect has been made in order to study the D layer adjustments to a solar eclipse (Barron, 1964). In such a case the vertical electric field is strongly inversly dependant on the effective ionospheric height.

SUMMARY

In reviewing the past work in this field and in our own contributions to the subject we have tried to show that the phenomenon of the Schumann resonances are reasonably well understood. This does not imply that the subject is closed, but rather, as we examine the parameters that are closely linked to the resonance behavior, it is evident that the subject should continue to provide important information concerning properties of the ionosphere that are difficult to obtain by other means. The two areas that are best suited to study by means of the Schumann resonances are the very low regions of the D layer, and the large scale picture of the geographic distribution of the ionospheric properties. In order to make fuller use of the information inherent in these signals, it will be necessary to have a broader geographical coverage of observing sites than exist at present. With a growing interest in this field, it is hoped that this situation will change.

Appendix A

Solutions of Wave-Guide Propagation Characteristics by the Matrizant Method

In section III it was shown that the full treatment of the earth-ionosphere wave-guide could be separated into two parts. The first part consisted of finding the TEM mode propagation characteristics of various segments of the wave-guide, and the second part consisted of fitting these segments together and studying the properties of the complete spherical waveguide. We wish to briefly outline here the method used for attacking the first part, and in appendix B we will outline the method used to do the second part.

In a given section the ionospheric parameters may be considered as being functions of altitude only. Because of the magnetic field, however, the equations still do not separate in spherical coordinates. Cylindrical coordinates however, allow the equations to separate and also keep the topological feature of the spherical surface, that the arc lengths vary in proportion to R. Thus assuming no Z dependance and an $e^{im\theta}$ dependance on θ we can write Maxwell's equations as

$$\frac{im}{r} E_z = j\mu\omega H_r \qquad \text{A-1}$$

$$\frac{dE_z}{dr} = -j\mu\omega H_\theta \qquad \text{A-2}$$

$$\frac{dE_\theta}{dr} + \frac{E_\theta}{r} - \frac{im}{r} E_r = j\mu\omega H_z \qquad \text{A-3}$$

$$\frac{dH_z}{dr} = -\sigma_{\theta\theta} E_\theta - \sigma_{\theta r} E_r - \sigma_{\theta z} E_z \qquad \text{A-4}$$

$$\frac{dH_\theta}{dr} + \frac{H_\theta}{r} - \frac{imH_r}{r} = \sigma_{zz} E_z + \sigma_{zr} E_r + \sigma_{z\theta} E_\theta \qquad \text{A-5}$$

$$\frac{imH_z}{r} = \sigma_{rr} E_r + \sigma_{r\theta} E_\theta + \sigma_{rz} E_z \qquad \text{A-6}$$

The displacement contribution, $-i\epsilon\omega$ is included in the value of the diagonal conductivity terms σ_{rr}, $\sigma_{\theta\theta}$, σ_{zz}. Eliminating Er and Hr from these equations we can write the four remaining equations as

$$\frac{dX}{dr} = -AX \qquad \text{A-7}$$

$$X = \begin{bmatrix} E_\theta \\ H_z \\ E_z \\ H_\theta \end{bmatrix} \qquad \text{A-8}$$

$$A = \begin{bmatrix} \frac{1}{r}\left(1 + \frac{im\sigma_{r\theta}}{\sigma_{rr}}\right) & \left(\frac{m^2}{r^2\sigma_{rr}} - i\mu\omega\right) & \left(\frac{im\sigma_{rz}}{r\sigma_{rr}}\right) & (0) \\ \left(\sigma_{\theta\theta} - \frac{\sigma_{\theta r}\sigma_{r\theta}}{\sigma_{rr}}\right) & \left(\frac{im\sigma_{\theta r}}{r\sigma_{rr}}\right) & \left(\sigma_{\theta z} - \frac{\sigma_{\theta r}\sigma_{rz}}{\sigma_{rr}}\right) & (0) \\ (0) & (0) & (0) & (i\mu\omega) \\ -\left(\sigma_{z\theta} - \frac{\sigma_{zr}\sigma_{r\theta}}{\sigma_{rr}}\right) & \left(-\frac{im\sigma_{rz}}{r\sigma_{rr}}\right) & \left(\frac{\sigma_{zr}\sigma_{rz}}{\sigma_{rr}} - \frac{im^2}{\mu\omega r^2}\right) & \left(\frac{1}{r}\right) \end{bmatrix} \qquad \text{A-9}$$

A convenient method of integrating these equations involves the use of matrizants (Fraser, Duncan and Collar, 1938; Gantmacher, 1960). A formal solution of A-7 is given as

$$X(r) = \Omega_{r_0}^{r} X(r_0) \qquad \text{A-10}$$

If $x(r_0)$ is known or if a combination of elements of $x(r)$ and $x(r_0)$ are known, a knowledge of $\Omega_{r_0}^{r}$ allows one to solve for the remaining term. In a waveguide problem the boundary impedances give one ratios of the elements of X, and then A-10 becomes a characteristic value problem to be solved for the characteristic wave numbers.

$\Omega_{r_0}^{r}$ is called the matrizant and it may be determined by an iterative integral procedure

$$\Omega_{r_0}^{r} = I + \int_{r_0}^{r} A(r_1)\,dr_1 + \int_{r_0}^{r} A(r_1) \int_{r_0}^{r_1} A(r_2)\,dr_2\,dr_1 + \cdots \qquad \text{A-11}$$

Also we have

$$\Omega_{r_0}^{r} = \Omega_{r_0}^{r_1}\,\Omega_{r_1}^{r} \qquad \text{A-12}$$

If sources produce a discontinuity in X of S_1 at r_1 we have

$$X(r) = \Omega_{r_0}^{r} X(r_0) + \Omega_{r_1}^{r} S_1 \qquad \text{A-13}$$

In a region where A is constant the matrizant takes a simple form which can be verified by substitution

$$\Omega_{r_1}^{r_2} = e^{(r_1-r_2)A} = I + (r_1-r_2)A + \frac{(r_1-r_2)^2}{2!}A\cdot A + \frac{(r_1-r_2)^3}{3!}A\cdot A\cdot A + \cdots \quad \text{A-14}$$

A-14 is much more convenient for numerical computations than A-11. One method, therefore, of approximately determining the matrizant is to break up the matrizant into the contributions of zones as in A-12 and then treat each zone as a layer of constant properties so that A-14 can be used for calculation. This is essentially the layered media approach, but the use of the matrizant calculations is especially handy when the analytic form of the solutions in the layers are not known. The convergence of the layered media approach has been discussed by Ferraro (Ferraro, 1962).

As we mentioned before, a waveguide mode problem is usually approached as a characteristic value problem, but in the Schumann resonance problem we are dealing with essentially only one waveguide mode, so that we can take certain short cuts. If the one mode has a propagation constant given as

$$k = \alpha + i\beta \qquad \text{(per unit } \theta\text{)}$$

and if a source of $e^{im\theta}$ is imposed, the resulting waves will vary as

$$X \sim \frac{e^{im\theta}}{(m-\alpha)-i\beta}$$

If a solution is then determined numerically, the phase of the solution allows one to determine the ratio of $\beta:(m-\alpha)$, and the ratio of the energy fed by the source into the guide per unit θ to the energy flow along the guide gives 2β .

Appendix B

Two Dimensional Network Solutions

The simplest difference equation approximations of 2nd order partial differential equations or pairs of 1st order equations lead to relationships between the node points that can be interpreted as electric network equations. A great deal of literature exists on numerical methods of solving the equations that arise from potential problems. The most efficient method is the method of overrelaxation. This method is still very efficient when dealing with damped electromagnetic waves in conducting media, but little analysis exists to guide one towards the proper amount of overrelaxation (Cox, 1963). When one is dealing with essentially propagating waves the diagonal dominance of the matrix equations is lost and the convergence of the relaxation techniques break down, and one must consider other techniques. When one looks at the equations as network equations one is naturally led into a technique that is straightforward and still highly efficient. If the network under consideration was a one dimensional ladder, no electrical engineer would ever bother with simultaneous solutions, but instead he would systematically compute the input impedances starting at one end and working back to the beginning (Iron, 1959). The partial results could be saved and from these impedance values the solution to any given source

distribution would quickly follow.

The very same steps can be taken for two dimensional networks, but now each row of circuit elements plays the role of a single element in the ladder analogy. Matrix inverses must then be performed, but the matrix sizes are determined by the number of elements in a row rather than the total number of elements in the network.

The method is described in matrix language as partitioning and triangularization (Forsythe and Wasow, 1960).

For convenience the steps in the solution algorithm are repeated below

Given a network and current sources, J, and unknown voltages V

$$J = YV \qquad \text{B-1}$$

which we partition into rows

$$Y = \begin{bmatrix} A_1 & C_1 & 0 & \\ C_1 & A_2 & C_2 & \\ 0 & C_2 & A_3 & \\ & & & \ddots A_N \end{bmatrix}, \quad V = \begin{bmatrix} V_1 \\ V_2 \\ \vdots \end{bmatrix}, \quad J = \begin{bmatrix} J_1 \\ J_2 \\ \vdots \\ \vdots \end{bmatrix} \qquad \text{B-2}$$

$$A_n = \begin{bmatrix} a_1 & -c_1 & 0 & \\ -c_1 & a_2 & -c_2 & \\ 0 & -c_2 & a_3 & \\ & & & \ddots \end{bmatrix}, \quad J_n = [j_{n1}, j_{n2} \cdots] \qquad \text{B-3}$$

$$C_n = \begin{bmatrix} -b_{n1} & 0 & 0 \\ 0 & -b_{n2} & 0 \\ 0 & 0 & -b_{n3} \\ & & \ddots \end{bmatrix}, \quad V_n = \begin{bmatrix} v_{n1}, v_{n2} \cdots \end{bmatrix} \qquad \text{B-4}$$

The b's are the admittances of the circuit elements connecting the node points to the nodes of the rows above and below. The c's are the admittances of the circuit elements connecting the node points to the neighboring nodes on the same row. The a's represent the sum of all the admittances connected to the node, including the admittance from the node to circuit ground.

Decompose Y into triangular forms

$$Y = EF \qquad \text{B-5}$$

$$E = \begin{bmatrix} I & 0 & 0 \\ E_1 & I & 0 \\ 0 & E_2 & I \\ & & \ddots \end{bmatrix}, \quad F = \begin{bmatrix} F_1 & G_1 & 0 \\ 0 & F_2 & G_2 \\ 0 & 0 & F_3 \\ & & \ddots \end{bmatrix} \qquad \text{B-6}$$

$$\therefore \quad E_n F_n = C_n$$
$$G_n = C_n \qquad \text{B-7}$$
$$E_n G_n + F_{n+1} = A_{n+1}$$

Starting with $F_1 = A_1$ the elements of E and F can be obtained by the algorithm

$$G_n = C_n$$
$$E_n = C_n F_n^{-1} \qquad \text{B-8}$$
$$F_{n+1} = A_{n+1} - E_n G_n$$

$$\text{Let} \quad FV = Z = \begin{bmatrix} z_1 \\ z_2 \\ \vdots \\ \cdot \end{bmatrix} \qquad \text{B-9}$$

Then B-1 can be written as

$$J = EZ \qquad \text{B-10}$$

Because of the simple form of E we can easily obtain Z as

$$Z_1 = J_1 \ , \ Z_n = J_n - E_{n-1} Z_{n-1} \qquad \text{B-11}$$

The final step of solving for V from Z also follows directly

The last element $V_N = F_N^{-1} Z_N$

The rest of the elements follow as

$$V_n = F_n^{-1}\left(Z_n - G_n V_{n+1}\right) \qquad \text{B-12}$$

F_n^{-1} has already been computed in B-8

The elements of E_n and F_n^{-1} can also be saved as a sort of Green's function for solving the same network with a new set of current sources.

Appendix C

Discussion of the Sources of Errors in the Computations

There are three types of errors inherent in the numerical results presented in this review. The first type results from errors in the physical laws used to set up the theoretical models. The only significant error in the theory that has been used here involves the simplification inherent in treating particle interactions in terms of an effective collision frequency. The actual particle interactions are not known well enough to allow one to analyse the effect of this error completely, but it appears that most of the effect can be taken into account by making the collision parameters slightly frequency dependant. If this is the case the effect of this error is lost in the second type of error, that due to improper models for the spacial distribution of the important physical parameters. In the long run the errors due to this second type will become the data which will be used to correct our models. This cannot be done, however, until the third type of error has been eliminated, that due to the mathematical approximations used to obtain numerical results. It is these errors which we wish to re-examine here. These errors include the errors of a layered approximation, the neglect of TE modes and higher order waveguide modes, the neglect of energy returning from the exosphere, and the errors of the network approximation.

It is known that the layered media approximation converges to the correct behavior as the number of layers becomes infinite, so that an empirical method of testing these errors is to carry through the computations for thinner and thinner layers and study the convergence. In our computations the layer thicknesses were distributed semi-logarithmically, the layering being cruder at the higher levels. Thus a nightime model would extend to 300 KM and for 20 layers the lowest layers were about 5 KM thick, and the highest layers, 30 KM thick. The ionosphere above 300 KM was assumed homogeneous. Each layer was assumed to have the properties associated with the middle of the layer. At around 8 cycles per second even a 20 layer model was close to the assymptotic behavior, and it is reasonable to expect the errors are within about 1%. In Table C-1 the behavior of the solution for an increasing number of layers is shown.

TABLE C-1

Effect of Number of Layers on Computed Propagation Characteristics Nightime Model

No. of layers	U/c	Q
20	.765	2.44
30	.775	2.28
40	.770	2.32

The errors involved with varying the height to the last layer were of a comparable magnitude. In the daytime, however, this height was set by the absorption properties of the ionosphere. If the height was extended too far, the solutions

became unstable because of round-off errors. This situation could be monitored from the partial results.

The neglect of all but the TEM mode was a basic concept in the treatment of the inhomogeneous earth-ionosphere waveguide. On theoretical grounds this was well justified because of the severe damping of these other modes. Some check on this was provided by the cylindrical models which did not inhibit these modes. The effect of the higher order waveguide modes could not be discerned in the solutions. The presence of a TE mode was discernable, but its energy was also insignificant.

Since 30 per cent of the energy escaped out of the cavity at night, and since the model did not account for any of this energy returning, some concern could arise about the errors of neglecting this energy. To test this source of error models were set up where this energy was all reflected back. It was found that the phase velocities were changed by as much as 4 per cent and the Q's increased from 5 to 30 per cent. Since only a fraction of the energy would actually return, and since the coherency of this energy would be lessened by variations of its slow path through the exosphere, and since only the night side is involved, it is reasonable to consider this error as not more than 1 per cent.

The lumped circuit network approximation of the transmission surface equations represented a significant source

of error. For a 10° x 20° model the resonant frequencies were in error by 1, 2 and 3 per cent for the first three modes. A correction factor was therefore applied to the resonance properties that were computed. The amplitude values would show even larger errors, and little significance could be given to any values within about 20 degrees of the source. Again correction factors could be devised to improve the results. The overall confidence in the numerical results quoted here is about comparable to that of the experimental results and appears to be adequate for the present.

ACKNOWLEDGEMENTS

We were first interested in the subject of the Schumann resonances through our contacts with Dr. Martin Balser and Mr. Charles Wagner and their work at the Lincoln Laboratories. They have continued to supply us with facts and ideas about the phenomenon. We have also benefitted from discussions about the theoretical aspects of the problem with Dr. Janis Galejs and Dr. James Wait. Dr. Galejs' suggestion of waveguide impedance concepts proved to be an important breakthrough for our work. Professor Freeman Gilbert of the University of California, San Diego, is responsible for much of our knowledge of the treatment of multi-layered media wave propagation, including our introduction to the matrizant methods. Mr. Roy Greenfield has helped us with the problems of network solutions.

Much of this present work was done while one of the authors was visiting the Institute of Geophysics and Planetary Physics at the University of California, San Diego, and we are indebted to the university computation center for their help, and the stimulation of the Institute staff, especially Professor Freeman Gilbert and Professor George Backus. The manuscript was prepared by Barbara Cullum.

To all these people we express our thanks. We also wish to acknowledge the support for our work of the Office

of Naval Research, contract NR-371-401. The computations at U.C.S.D. were supported by a grant from the National Science Foundation, NSF G13575. One of the authors was supported in his thesis studies by the Research Laboratory for Electronics. Massachusetts Institute of Technology.

BIBLIOGRAPHY

Aarons, J., Low frequency electromagnetic radiation 10 to 900 c/s, J. Geophys. Research, 61, 647-661, 1956.

Allis, W. P., S. J. Buchsbaum, and A. Bers, Waves in Anisotropic Plasmas, M.I.T. Press, Cambridge, 1963.

Arnold and Pierce, The Ionosphere Below 100 km, a Simple Model, Research Memorandum No. 11, Stanford Research Institute, 1963.

Balser, M. and C. Wagner, Measurement of the spectrum of radio noise from 50 to 100 c/s, J. Research N.B.S., 64D, 415-418, 1960.

Balser, M. and C. Wagner, Observations of earth-ionosphere cavity resonances, Nature, 188, 638-641, 1960.

Balser, M. and C. Wagner, Diurnal power variations of the earth-ionosphere cavity modes and their relationship to worldwide thunderstorm activity, J. Geophys. Research, 67, 619-625, 1962.

Balser, M. and C. Wagner, On frequency variations of the earth-ionosphere cavity modes, J. Geophys. Research, 67, 4081-4083, 1962.

Balser, M. and C. Wagner, Effect of a high-altitude nuclear detonation on the earth-ionosphere cavity, J. Geophys. Research, 68, 4115-4118, 1963.

Barron
Barrett, paper presented at Boulder Conference on U.L.F., August, 1964.

Benoit, R. and A. Houri, Sur la mesure de la densite spectral d'un bruit en géophysique. Application à la cavite terre-ionosphere, C. R. Acad. Sci., Paris, 225, 2496-2498, 1962.

Bourdeau, R. L., E. C. Whipple, and J. F. Clark, Analytic and experimental conductivity between the stratosphere and the ionosphere, J. Geophys. Research, 64, 1363-1370, 1959.

Brekhovskiki, L. M., Waves in Layered Media, Academic Press, New York, 1960.

Bremmer, H., Terrestial Radio Waves, Elsevier Publishing Co., New York, 1949.

Chapman, F. W. and R. C. Macario, Propagation of audio frequency radio waves to great distances, Nature, 177, 930-933, 1956.

Chapman, F. W. and D. L. Jones, Earth-ionosphere cavity resonances and the propagation of extremely low frequency radio waves, Nature, 202, 654-657, 1964.

Cox, C., Private communication, 1963.

Crain, C. M. and P. Tamarkin, A note on the cause of sudden ionization anomalies in regions remote from high altitude nuclear bursts, J. Geophys. Research, 66, 35-39, 1961.

Dalgarno, A., Charged particles in the upper atmosphere, Annales de Geophys., 17, 16-49, 1961.

Fejer, J. A., The interaction of pulsed radio waves in the ionosphere, J. Atmos. Terr. Phys., 17, 322-332, 1955.

Ferraro, A. J., Multislab concept applied to radio-wave propagation in the ionosphere and its limit to the continuous ionosphere, J. Geophys. Research, 67, 3817-3822, 1962.

Forsythe, G. E. and W. R. Wasow, Finite Difference Methods for Partial Differential Equations, John Wiley and Sons, New York, 1960.

Frazer, R. A., W. J. Duncan and A. R. Collar, Elementary Matrices, MacMillan Company, New York, 1947.

Galejs, J., Terrestial extremely-low-frequency noise spectrum in the presence of exponential ionospheric conductivity profiles, J. Geophys. Research, 66, 2787-2792, 1961.

Galejs, J., A further note on terrestial extremely-low-frequency propagation in the presence of an isotropic ionosphere with an exponential conductivity height profile, J. Geophys. Research, 67, 2715-2728, 1962.

Galejs, J., ELF and VLF waves below an inhomogeneous anisotropic ionosphere, J. Research, N.B.S., 68D, 693-707, 1964.

Gantmacher, Matrix Theory, Vol. II, Chelsea Publishing Co., New York, 1960.

Gardner, F. F. and J. L. Pawsey, Study of the ionospheric D region using partial reflections, J. Atmos. Terr. Phys., 3, 321-344, 1953.

Gendrin, R. and R. Stefant, Enregistrement et analyse spectral des vibrations des très basse frequence du champ magnetique terrestre dans la gamme de 1 a 50 Hz., C. R. Acad. Sci. (Paris), 254, 1852-1854, 1962.

Gendrin, R. and R. Stefant, Effet de l'explosion thermonucleaire a tres haut altitude du 9 Juillet 1962 sur la resonances de la cavite terre-ionosphere, Resultats experimenteaux, C. R. Acad. Sci. (Paris), 2273-2275, 1962.

Gendrin, R. and R. Stefant, Effet de l'explosion thermonucleaire a tres haut altitude du 9 Juillet 1962 sur la resonances de la cavite terre-ionosphere, Interpretation, C. R. Acad. Sci. (Paris), 2493-2495, 1962.

Ginzburg, V. L., Propagation of Electromagnetic Waves in Plasma, Gordon and Breach Science Publishers, New York, 1961.

Gustafsson, G., A. Egeland, and J. Aarons, Audio-frequency electromagnetic radiation in the auroral zone, J. Geophys. Research, 65, 2749-2758, 1960.

Handbook of Geophysics, USAF, MacMillan Co., New York, 1960.

Harris, F. B. and R. L. Tanner, A method for the determination of lower ionospheric properties by means of field measurements on sferics, J. Research, N.B.S., 66D, 463-478, 1962.

Hepburn, F. and E. T. Pierce, Atmospherics with low frequency components, Nature, 171, 837-838, 1953.

Hill, E. L., Very low frequency radiation from lightning strokes, Proc. I.R.E. 45, 775-777, 1957.

Holzer, R. E. and D. E. Deal, Low audio-frequency electromagnetic signals of natural origin, Nature, 177, 536-537, 1956.

Holzer, R. E., World thunderstorm activity and extremely low frequency sferics, Recent Advances in Atmospheric Electricity, Ed. Smith, L. G., Permagon, New York, 599-602, 1958.

Jean, A. G., A. C. Murphy, J. R. Wait, and D. F. Wasmundt, Observed attenuation rates of ELF radio waves, J. Research N.B.S., 65D, 475-479, 1961.

Johnson, F. S., Satellite Environment Handbook, Stanford University Press, Stanford, 1961.

Latter, R. and R. E. LaLevier, Detection of ionization effects from nuclear explosions in space, J. Geophys. Research, 68, 1643-1666, 1963.

Lokken, J. E., J. A. Shand, Sir. C. S. Wright, L. H. Martin, N. M. Brice, and R. A. Helliwell, Stanford Pacific Naval Laboratory conjugate point experiment, Nature, 192, 319-320, 1961.

Kane, J. A., Re-evaluation of ionospheric electron densities and collision frequencies derived from rocket measurements of refractive index and alternation, NASA Technical Note D-503, 1960.

Kenney, J. F. and H. R. Willard, Ionospheric perturbations due to an impulsive neutron source, J. Geophys. Research, 68, 4645-4657, 1963.

Knetch, R. W., The distribution of electrons in the lower and middle ionosphere, preprint of paper presented at XIV URSI General Assembly, 1963.

König, H. L., Atmospherics geringster Frequenzer, Z. Angew. Phys., 11, 264-274, 1959.

Konig, H. L., E. Haine, and C. H. Antoniadis, Messung von Atmospherics geringster Frequenzer in Bonn, Z. Angew. Phys., 13, 364-367, 1961.

Kron, G., Tensors for Circuits, Dover Publishing, Inc., New York, 1959.

Large, M. I. and T. W. Wormell, Fluctuations in the vertical electric field in the frequency range from 1 c/s to 500 c/s, Recent Advances in Atmospheric Electricity, Ed. Smith, L. G., Permagon Press, New York, 603-607, 1958.

Maeda, H., A. J. Shirgaokar, M. Yasuhara, and Matsushita, On the geomagnetic effect of the Starfish high-altitude nuclear explosions, J. Geophys. Research, 69, 917-945, 1964.

Moler, W. F., ULF propagation effects of a D region layer produced by cosmic rays, J. Geophys. Research, 65, 1459-1468, 1960.

Moler, W. F., Private communication, 1964.

Montgomery, C. G., R. H. Dicke and E. M. Purcell, Principles of Microwave Circuits, McGraw-Hill Book Co., New York, 1948.

Nicolet, M. and A. C. Aikin, The formation of the D region of the ionosphere, J. Geophys. Research, 65, 1469-1483, 1960.

Odencrantz, F. K., P. Saint-Amand, and J. G. Moore, Zenith airglow observations during the high-altitude nuclear explosion of July 9, 1962, J. Geophys. Research, 67, 4091-4092, 1962.

Oelbermann, Jr., and J. M. Musser, An analogue method for determining neutron shadow-cone geometry for high altitude nuclear tests, J. Geophys. Research, 69, 3733-3740, 1964.

Pekeris, C. L., Theory of propagation of explosive sound in shallow water, Memoir 27, Geol. Soc. Amer., 1948.

Pierce, E. T., Some ELF phenomena, J. Research N.B.S., 64D, 383-386, 1960.

Pierce, E. T., The propagation of radio waves of frequency less than 1 K c/s, Proc. I.R.E., 48, 329-331, 1960.

Pierce, E. T., Excitation of earth-ionosphere cavity resonances by lightning flashes, J. Geophys. Research, 68, 4125-4127, 1963.

Polk, C. and F. Fitchen, Schumann resonances of the earth-ionosphere cavity - extremely low frequency reception at Kingston, R. I., J. Research, N.B.S., 66D, 313-318, 1962.

Raemer, H. R., On the extremely low frequency spectrum of the earth-ionosphere cavity response to electrical storms, J. Geophys. Research, 66, 1580-1583, 1961.

Raemer, H. R., On the spectrum of terrestrial radio noise at extremely low frequencies, J. Research N.B.S., 65D, 581-593, 1961.

Ratcliffe, J. A., Editor, Physics of the Upper Atmosphere, Academic Press, New York, 1959.

Reid, G. C., Physical processes in the D region of the ionosphere, Reviews of Geophys. 2, 311-334, 1964.

Row, R. V., On the electromagnetic resonant frequencies of the earth-ionosphere cavity, IRE Trans. on antennas and propagation, AP-10, 766-769, 1962.

Rycroft, M. J., Low frequency disturbances of natural origin of the electric and magnetic fields of the earth, Ph.D. Thesis, University of Cambridge, 1963.

Schumann, W. O., Uber die strahlunglosen Eigenschwingungen einer leitenden Kugel, die von einer Luftschicht und einer Ionospharenhulle ungenben ist, Z Naturforschg., 7A, 149-154, 1952.

Schumann, W. O., Uber die Dampfung der elektromagnetischen eigenschwingungen des Systems Erde-Luft-Ionosphare, Z. Naturforschg, 7A, 250-252, 1952.

Schumann, W. O., Uber die Ausbreitong sehr langer elektrischer Wellen um die Erde und die Signale des Blitzes, Nuovo Cimento, 9, 1116-1138, 1952.

Schumann, W. O. and H. Konig, Uber die Beobachtung von atmospherics bei geringsten Frequenzen, Naturwiss, 41, 183-184, 1954.

Schumann, W. O., Uber elektrische Eigenschwingungen des Hohlraumes Erde-Luft-Ionosphare, erregt durch Blitzentladungen, Z. Angew, Phys., 9, 373-378, 1957.

Slater, J. C., Microwave Transmission, Dover Publications, Inc., New York, 1959.

Stefant, R., Application d'un magnetometre a induction a la detection des frequences de resonance de la cavite terre-ionosphere, Annales de Geophys., 19, 250-283, 1963.

Stix, T. H., The Theory of Plasma Waves, McGraw-Hill Book Co. New York, 1962.

Tepley, L. R., A comparison of sferics as observed in the VLF and ELF bands, J. Geophys. Research, 64, 2315-2329, 1959.

Tepley, L. R., Sferics from intracloud lightning strokes, J. Geophys. Research, 66, 111-123, 1961.

Thompson, W., A layered model approach to the earth-ionosphere cavity resonance problem, Ph.D. Thesis, M.I.T., 1963.

Wagner, C., Private Communication, 1963.

Wait, J. R., Terrestial propagation of very low frequency radio waves: a theoretical investigation, J. Research N.B.S., 64D, 153-204, 1960.

Wait, J. R., On the propagation of ELF radio waves and the influence of a non homogeneous ionosphere, J. Geophys. Research, 65, 597-600, 1960.

Wait, J. R., Mode theory and the propagation of ELF radio waves, J. Research N.B.S., 64D, [illegible], 1960.

Wait, J. R., A note concerning the excitation of ELF electromagnetic waves, J. Research N.B.S., 65D, 481-484, 1961.

Wait, J. R., Electromagnetic Waves in Stratified Media, Permagon Press, New York, 1962.

Wait, J. R., Review of mode theory of radio propagation in terrestial waveguides, Reviews of Geophys., 1, 481-536, 1963.

Wait, J. R., On the theory of Schumann resonances in the earth-ionosphere cavity, Can. Jour. Phys., [illegible], 575-582, 1964.

Wait, J. R., Two-dimensional treatment of mode theory of the propagation of VLF radio waves, J. Research N.B.S., 68D, 81-93, 1964a.

Watson, G. N., The diffraction of radio waves by the earth, Proc. Roy. Soc. London, 95A, 83-99, 1918.

Watson, G. N., The transmission of electric waves around the earth, Proc. Roy. Soc. London, 95A, 546-563, 1919.

Watt, A. D., ELF electric fields from thunderstorms, J. Research N.B.S., 64D, 425-433, 1960.

Weber, W., The production of free electrons in the ionospheric D layer by solar and galactic cosmic rays and the resultant absorption of radio waves, J. Geophys. Research, 67, 5091-5106, 1962.

Whipple, E. C., Jr., Electricity is the terrestial atmosphere above the exchange layer, NASA Technical Note, NASA TN D-2092, 1964.

Williams, H. P., The effect of high altitude nuclear explosions on radio communications, IRE Trans. on military electronics, 4, 326, 1962.

Willis, H. F., Audio-frequency magnetic fluctuations, Nature, 161, 887-888, 1948.

Wormel, T. W., Atmospheric electricity; some recent trends and problems, Quart. J. Roy. Met. Soc., 79, 3-38, 1953.

Zmuda, A. J., B. W. Shaw and C. R. Haave, Very low frequency disturbances and the high-altitude nuclear explosion of July 9, 1962, J. Geophys. Research, 68, 745-758, 1963.